MDPI

Review

Power Generation with Renewable Energy and Advanced Supercritical CO₂ Thermodynamic Power Cycles: A Review

Xinyu Zhang and Yunting Ge *

School of the Built Environment and Architecture, London South Bank University, 103 Borough Road, London SE1 0AA, UK; zhangx26@lsbu.ac.uk
* Correspondence: yunting.ge@lsbu.ac.uk

Abstract: Supercritical CO₂ (S-CO₂) thermodynamic power cycles have been considerably investigated in the applications of fossil fuel and nuclear power generation systems, considering their superior characteristics such as compactness, sustainability, cost-effectiveness, environmentally friendly working fluid and high thermal efficiency. They can be potentially integrated and applied with various renewable energy systems for low-carbon power generation, so extensive studies in these areas have also been conducted substantially. However, there is a shortage of reviews that specifically concentrate on the integrations of S-CO₂ with renewable energy, encompassing biomass, solar, geothermal and waste heat. It is thus necessary to provide an update and overview of the development of S-CO₂ renewable energy systems and identify technology and integration opportunities for different types of renewable resources. Correspondingly, this paper not only summarizes the advantages of CO₂ working fluid, design layouts of S-CO₂ cycles and classifications of renewable energies to be integrated but also reviews the recent research activities and studies carried out worldwide on advanced S-CO₂ power cycles with renewable energy. Moreover, the performance and development of various systems are well grouped and discussed.

Keywords: CO₂ working fluid; supercritical power cycles; renewable energy; advanced power generation systems; applications

1. Introduction and Motivation

Global energy demand is on the rise in numerous countries as the population increases and the economy grows. One of the primary and representative facts of economic growth in all countries worldwide is the increased electricity demand and generation. From 2019 to 2022, total primary energy consumption experienced a 3% increase, while the proportion of fossil fuel consumption in relation to primary energy consumption remained high at approximately 82% [1]. Growing energy consumption makes it a significant challenge to transition our energy sources and supplies away from fossil fuels and move towards low-carbon ones. Extensive fossil fuel consumption has caused environmental issues such as global warming, ozone depletion and atmospheric pollution. Therefore, it is critically important to achieve energy conversion efficiency improvement and increase renewable energy utilization and thus diminish the reliance on fossil fuels.

A decentralized and localized power generation system is an effective option to reduce energy consumption since energy loss from long-distance transmission or transportation can be avoided. Steam Rankine and gas turbine cycles have been significantly involved in large-scale power plants for electricity generation. The steam Rankine cycle can, however, achieve relatively higher energy conversion efficiency at lower turbine inlet temperature, considering the fact that the working fluid is pumped at a liquid state before being heated by a steam boiler. This is significant because liquid water is essentially incompressible, which can reduce the work required for pumping compared to compressing a gas by a compressor. According to the theory of the Carnot cycle for a heat engine, the higher

the temperature at which heat is supplied and the lower the temperature at which heat is rejected, the greater efficient the cycle will be. It reveals the importance of a power cycle operating at a higher heat supply temperature whenever possible to maximize its thermal efficiency. The gas turbine cycle, also known as the Brayton Cycle, utilizes air as a working fluid at a higher turbine inlet temperature. However, in the Brayton Cycle, the compression process consumes more work compared to the steam Rankine cycle since air is compressible. This leads to lower efficiency for the gas turbine cycle. On the other hand, over the last decades, as a mature energy conversion technology, the organic Rankine cycle (ORC) has been generally used in small-scale power generation. Industrial waste heat, biomass combustion, solar energy and geothermal heat can be utilized as heat sources for ORCs [2,3]. The ORC is superior to the traditional steam Rankine cycle in terms of performance when employing a low-temperature heat source. However, the selection of a working fluid for an ORC is a challenge due to the fact that some organic compounds have high global warming potentials (GWPs). Therefore, the investigation of alternative working fluids in applicable power generation cycles attracted more attention [4,5]. CO_2 is a natural, non-toxic, non-flammable, abundant and zero ozone depletion potential (ODP) working fluid, making it a noteworthy competitive candidate to be utilized in a power generation system [6]. According to its low critical point, the CO_2 power cycle can easily extend to the supercritical region and turn it into a transcritical or supercritical CO_2 power cycle. The supercritical CO_2 (S-CO_2) power cycle was originally proposed as a format of partial condensation Brayton cycle by Sulzer [7] in 1940. A simple recuperated supercritical Brayton cycle was propositioned by Feher [8] in 1967, and thereafter, Angelino [9–11] conducted a thorough study of CO_2 power cycles. The S-CO_2 Brayton cycle integrates the strengths of the steam Rankine and the gas turbine cycles by compressing the working fluid in the incompressible region and achieving higher thermal efficiency at higher turbine inlet temperatures.

S-CO_2 power cycles equipped with advantages of simplicity, compactness, sustainability and cost-effectiveness have therefore been significantly researched for various applications, including fossil fuel power plants, nuclear power plants, and integrations with renewable energies. The existing power cycles, such as Rankine and gas turbine cycles, face the challenges of working fluid selections and less cycle thermal efficiencies. Driven by the better thermal performance of energy conversion systems, CO_2 has attracted more attention to be utilized as an alternative working fluid. Another reason is the lower critical temperature at 31 °C which enables CO_2 working fluid and its associated system to be applicable in a variety range of heat sources. A power cycle with CO_2 working fluid could be classified as either a direct or indirect Brayton cycle. The semi-closed direct-fire oxyfuel Brayton cycle was suitable for fossil fuel power generation systems, while the indirect Brayton cycle was adapted for applications involving nuclear and renewable energy sources [12]. There have been many studies investigating the applications of direct S-CO_2 cycles. A design was conceptualized by Le Moullec [13] for a coal-fired power plant with 90% post-combustion CO_2 capture. It showed that the cost of electricity and the cost of CO_2 reduction could be reduced by 15% and 45%, respectively. Mecheri and Le Moullec [14] conducted additional simulations on S-CO_2 coal-fired power plants, concluding that by combining a coal-fired power plant with a double reheated single recompression Brayton cycle, a net thermal efficiency of 47.8% could be attained. This efficiency was significantly higher than that of traditional coal-fired power plants. Xu et al. [15] reached a similar conclusion, stating that the net power generation efficiency of a triple-compression S-CO_2 cycle could attain 49.01%, compared to 48.12% achieved by the water–steam Rankine cycle. In addition, although the fabrication cost could be increased, the levelized cost of electricity achieved a reduction of 1.32% compared to the water–steam Rankine cycle. Optimizing the recuperator in the system is crucial to reducing the total cost of the entire S-CO_2 cycle. To further enhance the performance of the S-CO_2 coal-fired power plant, employing a partial flow mode in the S-CO_2 boiler was demonstrated to effectively decrease pressure drop, thereby increasing the system's thermal efficiency [16]. As for the indirect Brayton

cycle, significant attention was paid to the $S-CO_2$ applications in nuclear reactors, as they could offer higher turbine inlet temperatures, potentially enhancing the system's thermal efficiency. Various countries have undertaken efforts to develop Generation IV nuclear reactors, given that these reactors operate in the temperature range of 500 °C to 900 °C, compared to water-cooled reactors with operating temperatures at around 300 °C [17]. Dostal [18] conducted an in-depth analysis of the $S-CO_2$ cycle for nuclear reactors. The study revealed that the $S-CO_2$ cycle exhibited competitive system efficiency compared to the helium Brayton cycle at the same operating condition. Additionally, it was concluded that the $S-CO_2$ power cycle was apt for all nuclear reactors with a core CO_2 gas heater outlet temperature exceeding 500 °C. Moisseytsev and Sienicki [19] investigated several alternative cycle layouts for $S-CO_2$ Brayton cycles coupled to the sodium-cooled fast reactor (SFR). It was found that no advantages could be gained from utilizing a double recompression cycle, incorporating intercooling between the main compressor stages or applying reheating between the high-pressure and low-pressure turbine cycles. However, optimizing the minimum cycle temperature down to 20 °C could lead to improvement in cycle efficiency. Wright et al. [20] demonstrated that integrating light water reactors (LWRs) with an $S-CO_2$ cycle could potentially improve the LWR power cycle efficiency and save capital costs. In order to further evaluate the benefits of coupling an $S-CO_2$ Brayton cycle with a small- and medium-sized water-cooled nuclear reactor (SWR), the effects of different operating conditions on system performance were studied by Yoon et al. [21]. The results revealed that even though the $S-CO_2$ cycle was previously recognized for having superior efficiency in high operating temperature regions, the efficiency of $S-CO_2$ with SMR cycle still demonstrated competitive efficiency to the existing steam-Rankine cycle with SMRs (around 30%) at the optimum pressure ratio. Additionally, a conclusion aligning with Wright [20] was reached that by combining the $S-CO_2$ cycle with SWR, capital costs could also be reduced. In 2021, about 440 nuclear power reactors were in operation in 32 countries worldwide with a total generated power of 2653 TWh, which took about 10% of the global electricity supply [22].

In light of growing environmental concerns, the utilization of the $S-CO_2$ power cycle in the renewable energy sector has recently emerged as an appealing option. While several researchers have provided extensive reviews of $S-CO_2$ cycles, as outlined in Table 1, the majority have focused on the development status of $S-CO_2$ cycles and the progress in optimizing components for applications in fossil fuel, nuclear, and solar power regions. Renewable energy resources are also known as alternative, sustainable or nonconventional energy supplies, including solar, geothermal, biomass and waste heat. However, reviews exclusively addressing $S-CO_2$ cycles in the context of these renewable energies are limited. Therefore, the objective of this paper is to review the most recent development of supercritical CO_2 cycles in power generation systems with renewable energy by offering a comprehensive view of the advantages of supercritical CO_2 working fluid, the landscapes of renewable energy, the options of $S-CO_2$ cycles, and application status of $S-CO_2$ renewable energies. Below are the key points highlighted in each section:

(i)   In Section 2, the superior thermal–physical properties of CO_2 are outlined, along with the benefits of incorporating CO_2 in supercritical power generation cycles.

(ii)   Section 3 demonstrates the advantage characteristics and categorizations of renewable energy as a promising source of heat, encompassing biomass, solar, geothermal and waste heat.

(iii) In Section 4, representative $S-CO_2$ cycles are summarized with emphasis on features of each layout, T-S diagrams and thermodynamic equations.

(iv)   In Section 5, a review of recent applications of $S-CO_2$ renewable power systems is presented, including $S-CO_2$ for biomass power systems, $S-CO_2$ cycle for concentrating solar power systems, $S-CO_2$ cycle for geothermal power systems and $S-CO_2$ cycle for waste heat recovery. This focuses on various technologies, operating conditions and efficiencies. In addition, the barriers to $S-CO_2$ technology are also concluded.

Table 1. Recent reviews on S-CO$_2$ power generation technologies.

Ref.	Year	Main Energy	Thermodynamic Equations	Summary Points	Limitations
Ahn et al. [17]	2015	• Coal-fired power plant • Nuclear • Waste heat recovery	n/a	• Performance of various layouts of S-CO$_2$ Braton cycles were compared. • Progress in the development of S-CO$_2$ was introduced.	Application reviews of various heat sources are not sufficient.
Kumar and Srinivasan [23]	2016	• Solar power	n/a	• The potential and limitation of thermodynamics were reviewed when CO$_2$ was used either alone or as a component in a mixture of the working fluid. • Heat transfer issue in recuperator was reviewed.	The study mainly focuses on the application of solar power generation without specifically considering other renewable energies.
Crespi et al. [24]	2017	• Nuclear • Solar power • Waste heat	n/a	• 42 standalone layouts of the S-CO$_2$ cycle and 38 combined cycle configurations were reviewed. • Operating conditions of different layouts were reviewed.	The limited thermodynamic equations or T-S diagrams aim to assist readers in comprehending distinctions among different S-CO$_2$ configurations.
Marchionni et al. [25]	2020	• Waste heat	n/a	• Technological challenges of high-grade waste heat recovery were reviewed. • Main components of S-CO$_2$ cycle were reviewed.	The illustrations of various cycles are not sufficient.
White et al. [26]	2021	• Fossil fuel • Nuclear • Solar power	n/a	• State-of-the-art S-CO$_2$ cycles, along with their technical and operational issues, were reviewed. • Development status of turbomachinery, heat exchanger, material selection and control system designs were reviewed.	The advantages of integrating the S-CO$_2$ cycle with renewable energies are not thoroughly outlined.
Guo et al. [27]	2022	• Coal-fired power plant • Nuclear • Solar power	n/a	• The challenges of state-of-the-art S-CO$_2$ technologies were reviewed. • Research progress of S-CO$_2$ power cycles and components was reviewed. • The review explores the thermodynamic, economic, environmental and flexible feasibility of the technology.	The thermodynamic performance of system application needs to be further analyzed.

2. Superior Thermal–Physical Properties of CO$_2$

CO$_2$ is a natural, non-toxic and non-flammable working fluid that possesses excellent thermophysical properties, including higher density, latent heat, specific heat, thermal conductivity and volumetric cooling capacity, along with lower viscosity [28]. These attributes make CO$_2$ a significant player in various energy conversion systems. It has a low critical temperature of 31 °C but quite a high critical pressure of 7.4 MPa. As shown in Figure 1, near the pseudocritical region, the thermophysical properties of CO$_2$ undergo rapid changes due to its high density and low compressibility factor close to its critical point. This leads to significant fluctuations in density and specific heat capacity with only

slight variations in pressure or temperature. The compressibility factor is characterized as the ratio of the actual volume of a substance to its ideal volume. As observed in Figure 2, around the critical point, the compressibility factor of CO_2 fluctuates between 0.2 and 0.5, which leads to a reduction in the power consumption of the compressor. Consequently, the S-CO_2 cycle is distinguished by its high thermal efficiency, simple cycle configuration and compactness of system components. At the same power generation, the overall size of a steam Rankine cycle is estimated to be approximately four times larger than that of an S-CO_2 Brayton cycle [17]. The benefits of utilizing CO_2 working fluid in thermodynamic cycles include (1) environmentally friendly nature, with no ozone-depleting potential (ODP) and neglectable global warming potential (GWP = 1), (2) abundance, non-toxicity and non-combustibility, (3) non-reactivity with component materials, and (4) superb thermodynamic and transport properties. According to the low critical temperature of CO_2 working fluid, its associated thermodynamic cycle can easily traverse both subcritical and supercritical regions with high-temperature heat sources, naming the cycles as either transcritical or supercritical cycles. Three options exist for utilizing CO_2 in the Brayton cycle as shown in Figure 3: (1) the classic cycle ('SN'), which operates entirely under critical pressure, known as the subcritical cycle; (2) the transcritical cycle ('TN'), the highest pressure operates above critical pressure, allowing CO_2 to pass through both subcritical and supercritical regions; and (3) the supercritical cycle ('S'), which operates entirely above the critical pressure. However, the difference between the transcritical and supercritical Rankine cycles is not strict. The transcritical Rankine cycle, under some conditions, can also be called the supercritical Rankine cycle. The concept of the supercritical CO_2 Rankine cycle pertains to the situation where heat addition happens at CO_2 pressure above the critical point, while heat rejection occurs at CO_2 pressure below the critical point, as illustrated in Figure 4. It has been demonstrated that the efficiency of the S-CO_2 Brayton cycle surpasses that of the superheated steam Rankine cycle when the turbine inlet temperature exceeds 470 °C [29]. The potential for maximizing power output in an ORC is hindered by the evaporation process with constant temperature, making it a less favourable option for sensible heat sources. By avoiding the isothermal boiling process, CO_2 in the transcritical/supercritical cycle achieves a more effective thermal match with the heat source, thereby attaining higher thermal efficiency compared to ORC, as depicted in Figure 5. The issue of pinching points between the heat source and working fluid temperature along the heat exchanger is effectively addressed by utilizing a transcritical or supercritical CO_2 cycle.
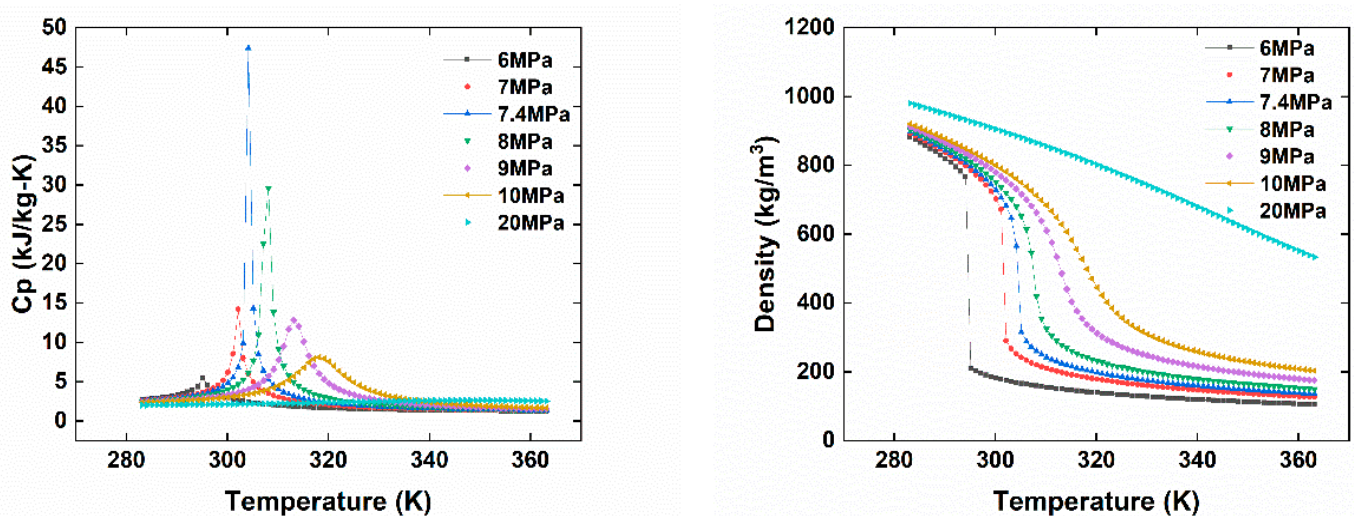
Figure 1. CO_2 thermal–physical properties vary with temperature at different pressures.
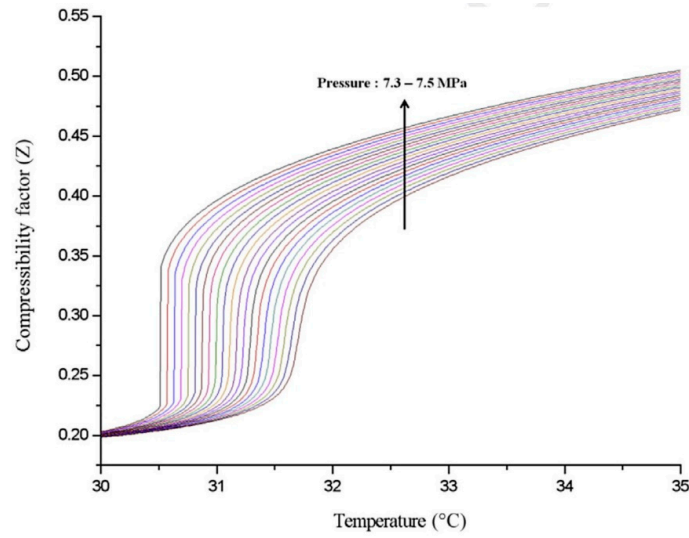
Figure 2. CO_2 compressibility factor [17].

Figure 3. P-H diagram and T-S diagram of subcritical, transcritical and supercritical CO_2 Brayton cycles: SN–subcritical; TN–transcritical; S–supercritical [30].

Figure 4. Configuration and processes of a CO_2 supercritical Rankine cycle. (**a**) The configuration. (**b**) The process in a T–S diagram [31].

Figure 5. Diagram illustrating the heat transfer between the heat source and working fluid in the high-temperature main heat exchanger: (**a**) ORC cycle. (**b**) CO_2 transcritical/supercritical power cycle [32].
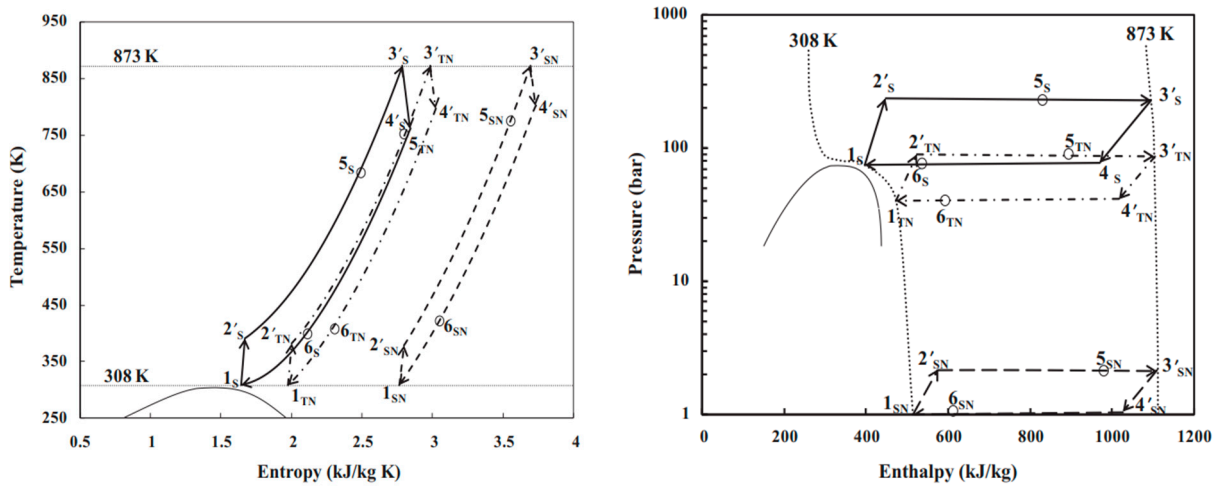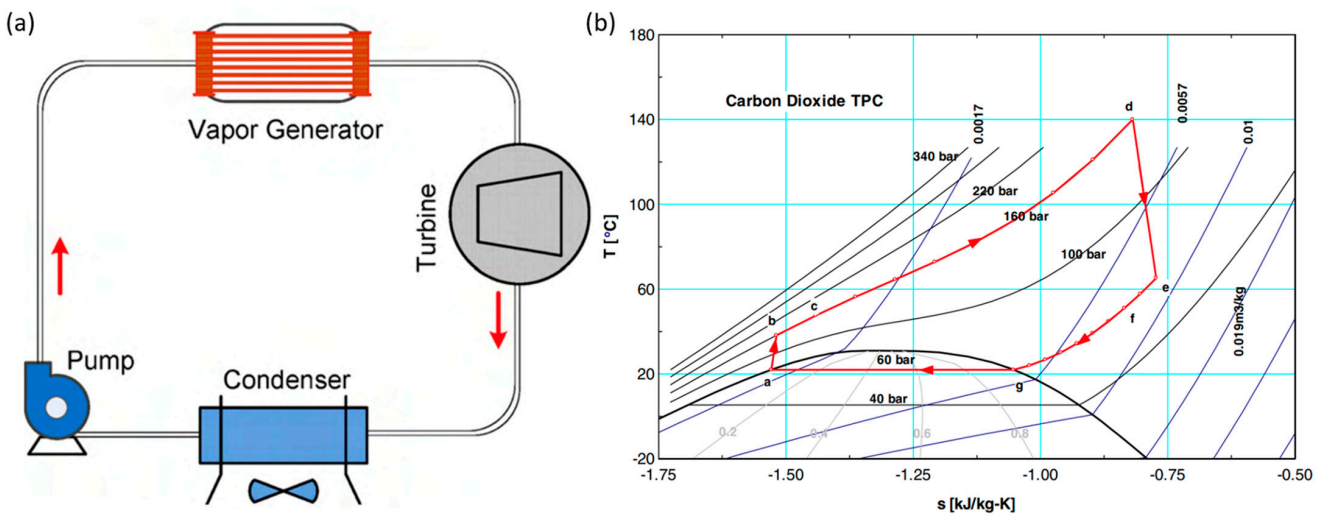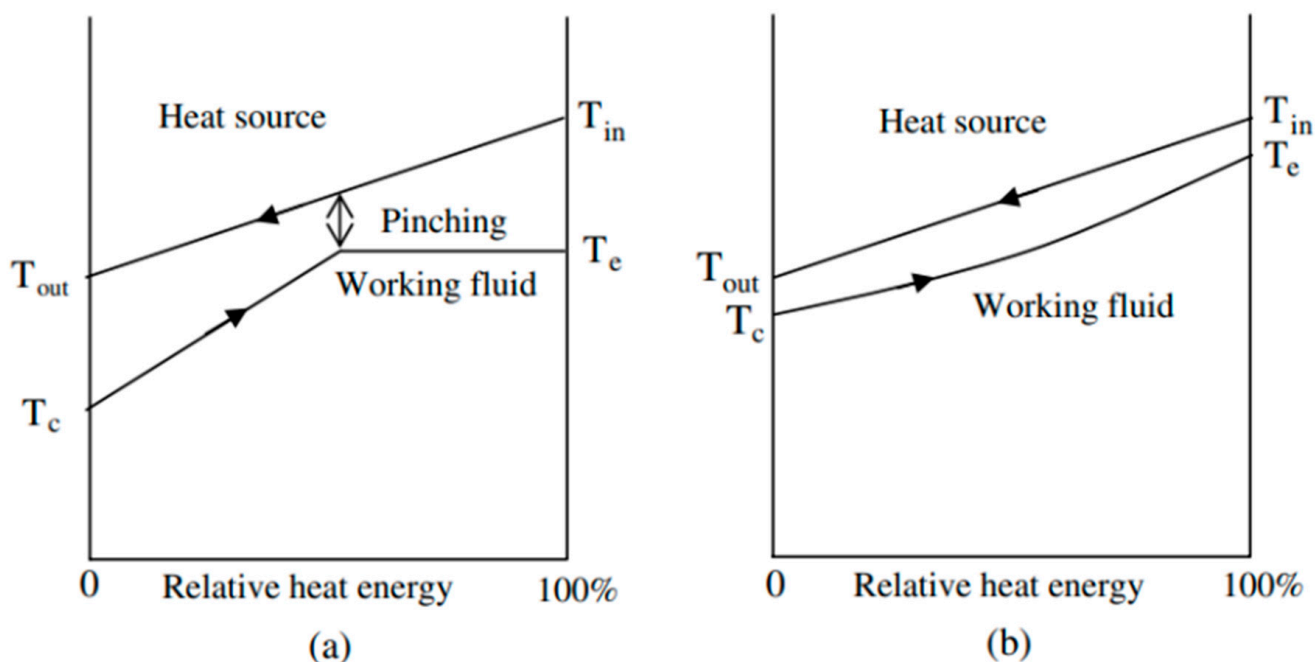
3. Superior Characteristics of Renewable Energy

3.1. Biomass

Biomass, a type of non-fossilized and biodegradable organic material originating from plants, animals and microorganisms, has emerged as a global frontrunner for the development of low-carbon energy. It encompasses products, by-products, residues and waste from agriculture, industry and forestry. The energy stored in biomass is initially derived from the sun, with photosynthesis being the primary process through which plants convert the sun's radiant energy into chemical energy, stored as glucose or sugar. Biomass is categorized into two main groups: virgin biomass, which includes forest biomass, energy crops and grasses; and waste biomass, which comprises municipal solid waste, agricultural crop residues and leaves [33]. Serving as a renewable and sustainable energy source, biomass can be utilized to generate electricity or other forms of energy. Unlike fossil fuels, the CO_2 produced from the complete combustion of biomass is equivalent to the amount it absorbs from the atmosphere, resulting in no net contribution to atmospheric carbon dioxide levels and emitting low levels of SOx and NOx. There are two main thermochemical conversion routes to use biomass for supplying electricity and heating, i.e., gasification and combustion. Combustion is the most mature technology to convert biomass to useful electricity and heating. Using biomass as a heat source can not only effectively reduce biomass waste but also provide high temperatures definitely higher than 900 °C [34] during the combustion process. Figure 6 shows the biomass energy conversion processes and temperature ranges of the thermochemical route.

Biomass has already become a crucial element in the UK's energy supply, contributing to 11% of the total electricity generated in 2022. According to the most recent energy statistics from the same year, it was estimated that bioenergy made up approximately 8.6% of the UK's overall energy supply [35]. The key advantages and disadvantages of biomass applications are outlined in Table 2 below.
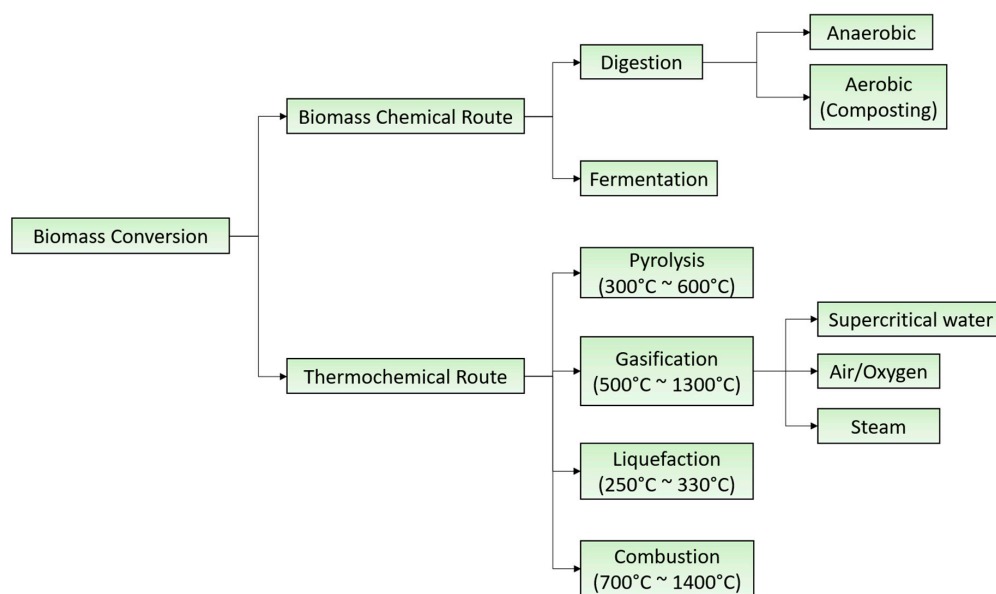
Figure 6. Biomass energy conversion processes.

Table 2. Major advantages and disadvantages of biomass.

Advantages	Disadvantages
Renewable and inexhaustible source	Low energy density
Low content of ash, C, S, N and trace elements	Potential competition with food and feed production
During combustion, ash can capture some hazardous components	Great harvesting, collection, transportation and storage cost
Cheap resource	Could lead to global warming if burned directly

3.2. Solar Power

Solar energy is the most abundant and widely distributed form of renewable energy available for utilization. Out of the 1.75×10^5 terawatts (TW) representing the total energy from the sun reaching Earth's atmosphere, approximately 1×10^5 TW consistently reaches the Earth's surface [36]. In 2022, solar energy production reached a total of 1289.27 terawatt-hours (TWh), contributing to approximately 4.6% of the global electricity generation [37].

There are two approaches to converting solar energy for electricity generation: the photovoltaic (PV) cell system and the solar thermal system. Generally, multiple PV cells are linked in a series to capture sunlight and transform it into direct current (DC) electrical power. Nevertheless, PV systems are primarily employed on a smaller scale and can be affected by weather conditions. In contrast, solar thermal systems are suitable for larger-scale applications. Conventional concentrating solar power (CSP) is a well-known sunlight conversion technology. Typically, a CSP consists of a central receiver system, parabolic trough, dish Stirling unit and integrated gas cycles. The CSP plant generates electricity by using a linear or punctual collector to focus on radiation energy and convert it into high-temperature heat. This high-temperature heat is then transferred into a working fluid, and the absorbed heat is thus converted into electricity by a generator via a power cycle. The Rankine cycle is the most common technology for converting solar energy to electricity [38]. The main components of a solar ORC system are the solar collector and evaporator, energy storage, turbine, generator and condenser, as shown in Figure 7. However, as explained previously, the ORC is more appropriate for low-temperature heat sources [39]. In addition, oil, salt and steam are typical heat transfer fluids used in CSP systems for converting solar energy into electricity. Nevertheless, the properties of these heat transfer mediums can impose constraints on the performance of CSP plants. For instance, synthetic oil and salt can only withstand temperatures up to 400 °C and 560 °C,

respectively, and direct steam generation has limitations in terms of storage capacity [40]. From the study of Dostal et al. [29], the S-CO$_2$ cycle outperformed the steam Rankine cycle when the inlet temperature of the turbine exceeded 550 °C. This temperature range falls within the attainable parameters of solar power systems, with the hot-end temperatures having reached between 800 °C and 1000 °C [41] or even above 1000 °C [42]. The challenges of the development of solar thermal power systems are the lower efficiency and high capital cost. As an alternative promising technology, the S-CO$_2$ cycle has become more favourable for converting solar power to electricity since it has higher thermal efficiency.
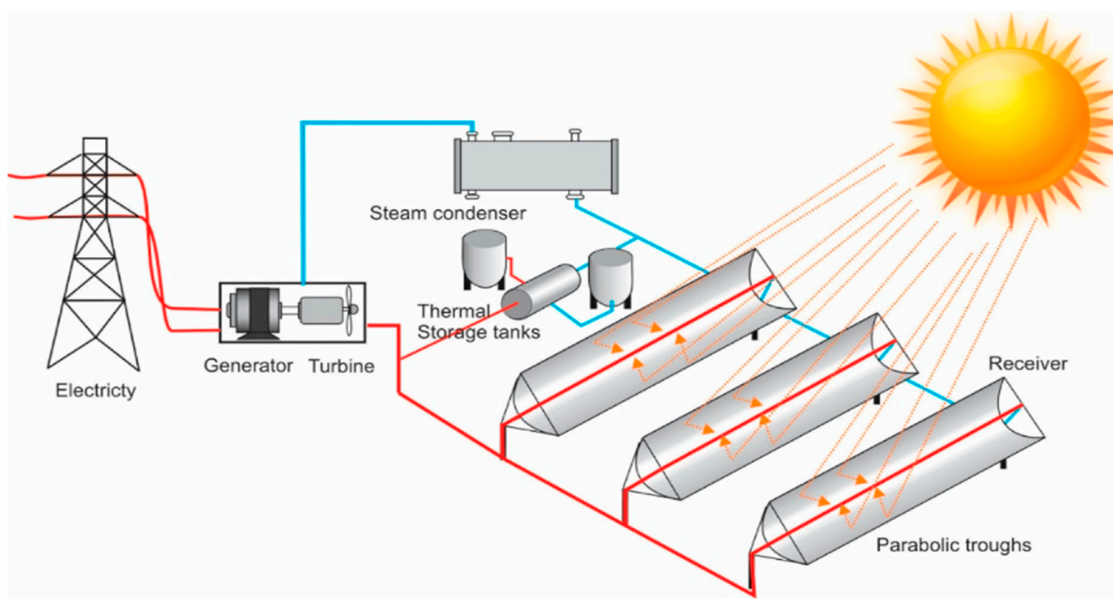
Figure 7. Solar thermal power generation system [43].

3.3. Geothermal Resource

Geothermal energy is globally available, constituting a clean, plentiful and sustainable energy source originating primarily from the natural decay of radioactive isotopes during the Earth's formation, deeply embedded within its layers. There is approximately 43,000,000 EJ of geothermal energy stored at depths reaching as far as 3000 m below the surface [44].

Hydrothermal resources represent the dominant form of geothermal energy harnessed for large-scale electricity generation. In addition to hydrothermal sources, there are five other categories of geothermal energy: hot dry rock, geopressured, magma energy, deep hydrothermal and low-temperature systems [45]. The temperature range of the geothermal heat resources is between 50 °C and 350 °C [46]. Geothermal resources can also be classified into various temperature grades, which are high-temperature (>180 °C), intermediate temperature (100–180 °C) and low-temperature (<100 °C) [39]. In order to extract heat at a suitable temperature, it is typically necessary to drill holes into the ground, creating both production and injection wells. Table 3 shows the potential of different heat source temperature ranges of geothermal energy in Europe.

Table 3. Potential of different heat source temperature ranges of geothermal energy in terms of heating (MW$_{th}$) and electricity (MW$_e$) in Europe [47].

Temperature °C	MW$_{th}$	MW$_e$
65–90	147,736	10,462
90–120	75,421	7503
120–150	22,819	1268
150–225	42,703	4745
225–350	66,897	11,150

3.4. Waste Heat Resource

Low-temperature exhaust stream emission is still a notable issue. In many manufacturing industries, 20~50% of the energy consumed by manufacturing is lost as waste heat [48]. However, this heat cannot be recovered completely on-site and used for district heating. It is then discharged into the ambient, which has a significant negative impact on human health, biodiversity, and the environment. Generally, waste heat can be categorized as low-temperature (<230 °C), medium-temperature (230–650 °C) and high-temperature (>650 °C) [3]. Recovery of low-grade waste heat for electricity production is a promising technology to protect the environment and meet electricity demand, although it is a big challenge for power plants. There are several technologies for waste heat recovery based on the heat transfer between working fluid and waste heat. The organic Rankine cycle is a common method utilized for low-grade waste heat recovery, in which heat is immediately recovered by a heat transfer loop to evaporate the working fluid. Persichilli et al. [11,25] discovered that the transcritical CO_2 power cycle could attain superior efficiency across a broad spectrum of heat source temperatures, ranging from 204 °C to 650 °C, and be more cost effective in comparison to ORC and steam Rankine cycles. Similarly, Chen et al. [32] conducted a comparative analysis between transcritical CO_2 Rankine and R123 ORC cycles, utilizing a low-grade heat source with a temperature of 150 °C. Their investigation established that the transcritical CO_2 cycle outperformed the subcritical R123 ORC one in terms of efficiency. However, for the low-grade heat source temperature of around 100 °C, the power output of the transcritical R125 cycle was approximately 14% higher than that of the transcritical CO_2 cycle. Moreover, if the heat temperature is as low as approximately 112 °C, the transcritical CO_2 Rankine cycle exhibits greater efficiency than that of the transcritical CO_2 Brayton cycle due to reduced compression work while achieving the same temperature increase. The supercritical CO_2 Brayton cycle is expected to replace the organic Rankine cycle to improve thermal efficiency for waste heat recovery. In addition, the S-CO_2 cycle can recover waste heat from small turbines.

4. S-CO_2 Layouts

The progressions of the five representative S-CO_2 cycles are delineated in Figure 8, including the recuperation cycle [8], recompression cycle [18,29,49,50], pre-compression cycle [10,51], intercooling cycle [52] and reheating cycle [53]. Various configurations have been explored to enhance the performance of S-CO_2 cycles, building upon the fundamental S-CO_2 power system depicted in Figure 8a. Thermodynamic equations of each component and thermal efficiencies of different layouts are summarized in Tables 4 and 5, respectively. The introduction of a recuperator allows for the recovery of more waste heat, resulting in what is termed the recuperation S-CO_2 cycle, as illustrated in Figure 8b. However, the adoption of an internal heat exchanger or recuperator, while boosting electrical efficiency, has revealed a significant internal irreversibility issue within the recuperator. This is primarily due to the substantial difference in specific heat capacity between the cold and hot fluid sides of CO_2, leading to a pinch-point problem [49]. The smaller the pinch-point, the better the heat transfer efficiency; however, a larger heat transfer area could be required. To address the pinch-point problem, a recompression S-CO_2 cycle was developed, as shown in Figure 8c. In this configuration, an additional recuperator and compressor are introduced. A portion of CO_2 is cooled by a gas cooler and then compressed to the highest pressure by the main compressor. The remaining amount of CO_2 is compressed by the secondary compressor. These two streams are combined at the inlet of the high-temperature recuperator (HTR or Recuperator 1) on the high-pressure side. This minimizes the temperature difference between the hot and cold fluid sides of CO_2, thereby improving heat transfer performance and resolving the pinch-point issue. Recompression S-CO_2 is the most efficient cycle compared to internal cooling, reheating and pre-compression cycles [18]. The pre-compression configuration offers an alternative method to mitigate the impact of the pinch-point problem and enhance regeneration, as seen in Figure 8d. The pre-compression cycle was initially introduced by Angelino [10]. It involves the placement of a

pre-compressor between the high-temperature recuperator (HTR) and the low-temperature recuperator (LTR or Recuperator 2). This pre-compression cycle works by narrowing the gap in specific heat capacity between the low-pressure and high-pressure streams via the elevation of pressure in the low-pressure stream. Intercooling is the traditional method to minimize the load of the compressor and increase the thermal efficiency of the S-CO$_2$ cycle. Increasing the number of stages results in the compression process approaching near-isothermal conditions at the compressor's inlet temperature [54]. However, intercooling (Figure 8e) does not hold much appeal in S-CO$_2$ cycles due to the minimal efficiency enhancement it provides [18]. Reheating (Figure 8f) is the technology to improve the turbine work and thus enhance the thermal efficiency of the S-CO$_2$ cycle since work output from the turbine could be increased without increasing the maximum temperature in the cycle and keeping the compressor work constant. Reheating holds substantial promise for the development of the S-CO$_2$ cycle. Nonetheless, it is exclusively applicable to indirect cycles, and utilizing more than one reheat stage is not economically practicable.
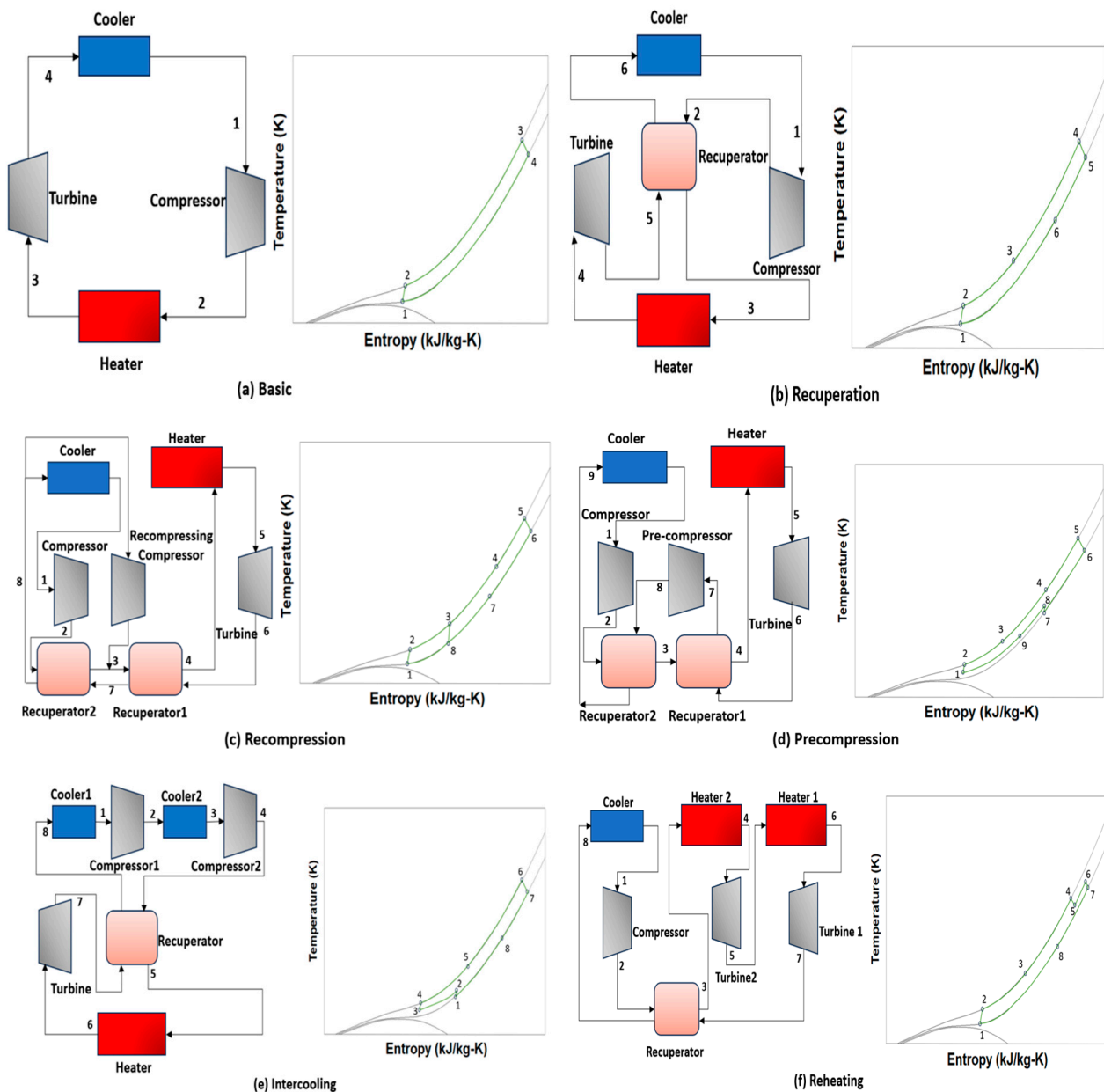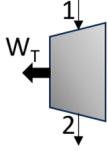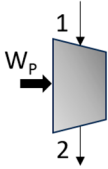

Figure 8. Layouts of S-CO$_2$ Brayton cycle and T-S diagrams.

Table 4. Thermodynamic equations of each component.

Component		Thermodynamic Equation
Heater		$Q_H = \dot{m}(h_4 - h_3)$
Turbine		$W_T = \dot{m}(h_1 - h_2),$ $\eta_T = (h_1 - h_2)/(h_1 - h_{2,s})$
Recuperator		$Q_{rec,max} = min\{ {\dot{m}(h_1-h_2),assumming\,T_2=T_3 \atop \dot{m}(h_4-h_3),assumming\,T_4=T_1} \}$ $\varepsilon_{rec} = \frac{h_1-h_2}{Q_{rec,max}} = \frac{h_4-h_3}{Q_{rec,max}}$
Gas cooler		$Q_c = \dot{m}(h_1 - h_2)$
Compressor		$W_P = \dot{m}(h_2 - h_1)$ $\eta_P = (h_{2,s} - h_1)/(h_2 - h_1)$

Table 5. Thermal efficiencies of each S-CO$_2$ layout.

Layout	First Law Efficiency Equation
Basic S-CO$_2$	$\eta_{th} = \frac{W_T - W_P}{Q_H}$
Recuperation S-CO$_2$	$\eta_{th} = \frac{W_T - W_P}{Q_H}$
Recompression S-CO$_2$	$\eta_{th} = \frac{W_T - \sum W_P}{Q_H} = \frac{W_T - (W_{compressor} + W_{re-compressor})}{Q_H}$
Pre-compression S-CO$_2$	$\eta_{th} = \frac{W_T - \sum W_P}{Q_H} = \frac{W_T - (W_{pre-compressor} + W_{compressor})}{Q_H}$
Intercooling S-CO$_2$	$\eta_{th} = \frac{W_T - \sum W_P}{Q_H} = \frac{W_T - (W_{P,1} + W_{P,2})}{Q_H}$
Reheating S-CO$_2$	$\eta_{th} = \frac{\sum W_T - W_P}{Q_{in}} = \frac{(W_{T,1} + W_{T,2}) - W_P}{Q_{H,1} + Q_{H,2}}$

5. Application Status of S-CO$_2$ Renewable Power Systems

5.1. S-CO$_2$ for Biomass Power Systems

Typical biomass power generation technologies have been listed in Table 6. Biomass can be combusted directly within waste-to-energy facilities for electricity production. Biomass co-firing is the substitution of a portion of the fuel with biomass within coal-fired thermal power plants. It is an economical approach to convert biomass effectively and environmentally into electricity and involves integrating biomass as a partial replacement for fuel in high-efficiency coal boilers [55]. Sweden has successfully operated the initial integrated gasification combined cycle (IGCC) plant that utilizes 100% biomass, specifically straw [56]. However, biomass poses a constraint on the adoption of large-scale steam cycles or IGCCs, which are designed to achieve higher efficiencies. The majority of biomass plants are typically small-scale and rely on internal combustion engines and ORCs. The electrical efficiency of a biomass-fired ORC system was between 7.5% and 13.5% [57]. Subsequently, in an experimental study conducted by Qiu et al. [58], it was observed that the electricity generation efficiency of this biomass-fired ORC system was 1.41%, primarily attributed to the lower efficiency of the expander and alternator during the experiments.

Table 6. Typical data for power generation from biomass [56].

Technologies	Efficiency % (LHV)	Typical Size (MWe)	Typical Costs	
			Capital Costs ($/kW)	Electricity ($/kWh)
Co-firing	35–40	10–50	1100–1300	0.05
Dedicated steam cycles	30–35	5–25	3000–5000	0.11
IGCC	30–40	10–30	2500–5500	0.11–0.13
Gasification + engine CHP	25–30	0.2–1	3000–4000	0.11
Stirling engine CHP	11–20	<0.1	5000–7000	0.13

For the further development of biomass conversion technologies, a supercritical CO_2 power system is a promising option for the efficient utilization of abundant renewable resources. Biomass has the potential to be used for power generation and bio-synthetic production with zero CO_2 emission. Chitsaz et al. [59] proposed a novel tri-generation system of bio-synthetic nature gas, fresh water and power, as illustrated in Figure 9. The operational concept of this system involves introducing biomass into the fluidized bed gasifier, where it undergoes a reaction with steam to produce a mixture of highly combustible species such as H_2, CO and CH_4. Subsequently, this high-temperature hydrogen-rich syngas flows through a CO_2 gas heater, elevating the temperature of CO_2 to drive the S-CO_2 Brayton cycle, and subsequently enters the methanation reactor. By utilizing heat from heat exchangers 3 and 4 within the humidification–dehumidification loop, seawater can be transformed into freshwater. By carrying out a comprehensive simulation of this system, it was found that the power production of 172.6 kW could be achieved under multi-objective optimum conditions. An alternative approach to utilize biomass gasification combined with the S-CO_2 Brayton power cycle is the combustion of biofuel. Cao et al. [60] introduced a heat and power system that integrates biomass gasification with an advanced solid oxide fuel cell-CO_2 supercritical Brayton cycle, as shown in Figure 10. After the biofuel (solid oxide fuel cell) is produced via the peach stone gasification process, it is burned in post-combustion to generate high-temperature gas up to 600 °C~700 °C. The results indicated that the optimal conditions for achieving maximum power (138 kW) and heat (195 kW) were as follows: an equivalence ratio of 4, a fuel cell temperature of 680 °C, a fuel utilization factor of 0.82 and a pressure ratio of 5.11. To enhance the electrical power output even further, biomass gasification with CHP plants can be equipped with multiple power cycles. Ji-chao and Sobhani [61] conducted a mathematical modelling study on an integrated power and heat system that merged biomass gasification with both the S-CO_2 Brayton cycle and the Kalina cycle. They achieved a peak net power output of 7.375 MW when the pressure ratio was set at 3.5. Moradi et al. [62] conducted a comparison study between a gas turbine and an S-CO_2 cycle, both of which were coupled with bottom ORCs and heated via biomass gasification. The results indicated that the average net electric power output of the entire integrated S-CO_2 system was approximately 126 kW, which was about 25% higher than the power output of the gas turbine system.

For the combustion biomass conversion route, a small-scale power generation test system with biomass and CO_2 transcritical Brayton cycles has been designed and constructed with purposely selected and manufactured system components [63–65], as depicted in Figure 11. Based on their modelling findings, it was discovered that there was an ideal pressure ratio that maximizes the thermal efficiency of the system. Furthermore, a higher temperature of the biomass flue gas was associated with higher thermal efficiency. As a single S-CO_2 cycle may utilize high-temperature flue gas insufficiently, a concept of cascaded supercritical CO_2 Brayton cycles was proposed to optimize the conversion efficiency of biomass energy into electricity, with a potential maximum efficiency of up to 36% [66]. Wang et al. [67] conducted a thermodynamic analysis of a biomass-solar combined with S-CO_2 Brayton power generation system. The combined use of solar energy and biomass enabled the continuous operation of the system. This is because biomass steps in to supply heat, either partially or entirely, when solar irradiation falls short. This system consists

of a solar island, a biomass burner, a recompression S-CO_2 cycle and a simple recuperation S-CO_2 cycle. Results showed that the solar-to-electric efficiency could achieve up to 27.85%. More studies of biomass energy conversion technologies based on S-CO_2 cycles have been summarized in Table 7. Although higher efficiency in biomass conversion to electricity can be obtained by using the supercritical CO_2 Brayton cycle, some barriers still exist for bioenergy development. The limited large-scale application of biomass can be attributed to several factors, including the need for logistics for feedstock collection and transportation, elevated feedstock costs compared to fossil fuels and greater upfront capital investment requirements.

Figure 9. A S-CO_2 biomass system for bio-synthetic natural gas, power and freshwater productions [59].

Figure 10. The integration of proton-conducting solid oxide fuel cell and supercritical CO_2 Brayton cycle [60].

Figure 11. A small-scale power generation and heat recovery test rig based on biomass with CO_2 transcritical Brayton cycle [64].

Table 7. Reviews in biomass conversion technologies.

Refs	Year	Biomass Conversion	Thermodynamic Cycle	Optimum Power Production (kWe)	Energy Conversion Efficiency
Manente et al. [66]	2014	Combustion	Cascaded supercritical CO_2 Brayton cycles	5359	36%
Wang et al. [67]	2018	Combustion	Recompression S-CO_2 Brayton cycle combined with Recuperation S-CO_2 Brayton cycle	11,250	21%
Ge et al. [63–65]	2020	Combustion	Recuperation T-CO_2 Brayton cycle	11.9	22%
Nkhonjera et al. [68]	2020	Gasification	Recuperation S-CO_2 Brayton cycle combined with Steam Rankine cycle	-	60%
Ji-chao et al. [61]	2021	Gasification	Recuperation S-CO_2 Brayton cycle combined with Kalina cycles	7400	78.15%
Chein et al. [69]	2021	Gasification	Recuperation S-CO_2 Brayton cycle	-	21%
Chitsaz et al. [59]	2022	Gasification	Recuperation S-CO_2 Brayton cycle	172.6	-

Table 7. *Cont.*

Refs	Year	Biomass Conversion	Thermodynamic Cycle	Optimum Power Production (kWe)	Energy Conversion Efficiency
Cao et al. [60]	2022	Gasification	Recuperation S-CO$_2$ Brayton cycle	138	-
Wang et al. [70]	2022	Gasification	semi-closed S-CO$_2$ cycle with a bottom ORC	70,210	38.76%
Moradi et al. [62]	2023	Gasification	Gas turbine, S-CO$_2$ Brayton cycle, ORC	126	48%
Zhang et al. [71]	2023	Gasification	Gas turbine cycle, S-CO$_2$ cycle, Organic Flash Cycle integrated	8210	75.80%
Zhang et al. [72]	2023	Gasification	Recuperation S-CO$_2$ Brayton cycle	68,200	67.98%

5.2. S-CO$_2$ Cycle for Concentrating Solar Power Systems

Globally, there are 144 concentrated solar power (CSP) projects running in 22 countries, where Spain, the United States and China are at the forefront in terms of construction and operation [73]. However, among those projects, steam Rankine cycles or organic Rankine cycles are still the primary technologies for converting solar energy to electricity. In comparison to photovoltaic (PV) panel technologies, CSP exhibits an inherent capacity to retain thermal energy for a short time, allowing for its subsequent conversion into electricity. CSP plants, when equipped with thermal storage capacity, have the capability to generate electrical power even in situations where sunlight is blocked by cloud cover or during post-sunset hours. CSP can be classified into three categories, including the first generation with a receiver temperature range of 250 °C~450 °C, the second generation with a receiver temperature range of 500 °C~720 °C, and the third generation with a receiver temperature above 700 °C. Moreover, based on the collector's type, CSP technologies can be divided into four types, including linear Fresnel reflector (LFR), solar power tower (SPT), parabolic power dish collector (PDC) and parabolic trough collector (PTC) [74], as illustrated in Figure 12. Detailed information regarding the CSP category is listed in Table 8.
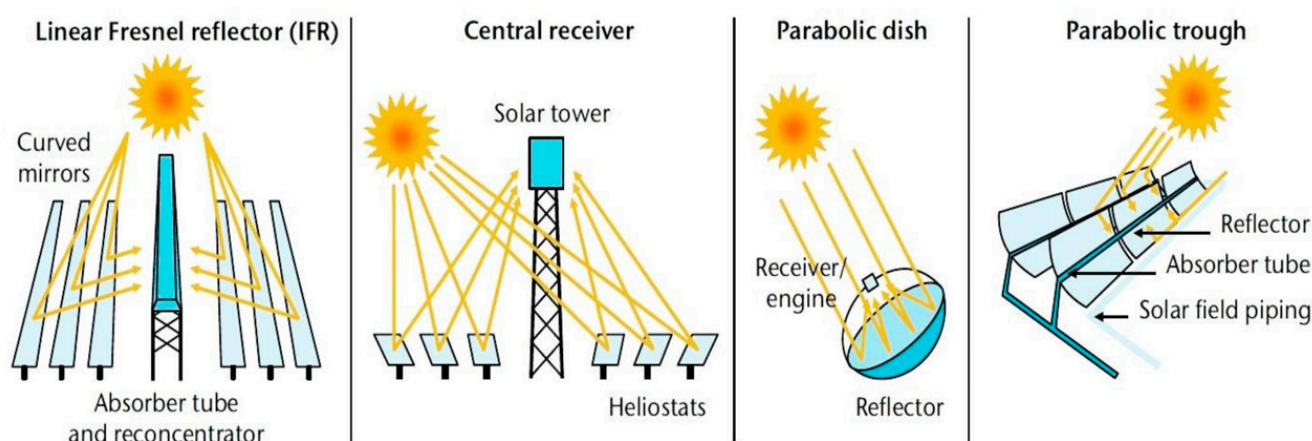

Figure 12. Main CSP technologies [75].

Table 8. Categories of CSP technologies [76].

Generation	First Generation	Second Generation	Third Generation
Receiver outlet temperature (°C)	250–450	500–720	>700
Typical technology	Parabolic trough collector Solar power tower Linear Fresnel reflector	Parabolic trough collector Solar power tower Linear Fresnel reflector Power dish collector	Particles Gas
Heat transfer medium	Oil Steam	Salt Steam Gas	Salt Air Helium CO_2
Thermodynamic cycle	Steam Rankine cycle	Steam Rankine cycle/Stirling	Brayton cycle
Cycle efficiency (%)	28–38	38–44	>50

The levelized cost of electricity (LCOE) is widely recognized as a crucial metric for assessing different power generation systems, as it encompasses all relevant aspects, such as initial capital investments, installation expenses, continuous operational costs and maintenance expenditures across the full lifespan of a power station [77]. The development of S-CO_2 technology in CSP applications is crucial for improving the efficiency of solar plants. Replacing the steam Rankine power block with an S-CO_2 cycle can enhance the LCOE of conventional molten salt tower technology. Operating at salt temperatures close to 600 °C is projected to yield an 8% enhancement in LCOE, while further advancements in temperature and efficiency can be achieved by employing S-CO_2 power cycles in CSP systems [78].

Comprehensive modelling of various SPT systems that are coupled with S-CO_2 Brayton cycles was conducted by Wang et al. [79]. Results showed that the intercooling cycle delivered the highest level of efficiency, with the partial-cooling cycle ranking the next, followed by the recompression cycle. Similarly, Neises and Turchi [80] concluded that the implementation of a partial cooling cycle had the potential to generate a larger temperature difference across the primary heat exchanger, thus leading to cost savings on the heat exchanger and enhancing the efficiency of the CSP receiver. Zhu et al. [81] further investigated the effects of different turbine inlet temperatures on the thermal efficiency of this system which was the same as Wang et al.'s [79]. The findings indicated that the turbine inlet temperature had a parabolic impact on the overall efficiencies of each S-CO_2 cycle. For further improving the efficiency of S-CO_2 SCP, modified cycles have been investigated at different operating conditions. The thermal efficiency of the supercritical CO_2 Brayton cycle consistently rises with the temperature of the cycle, as seen in Figure 13, by comparing with different S-CO_2 cycles, including recuperation, recompression, partial cooling with recompression and recompression with main compression. The recompression cycle with main compression intercooling achieved the best thermal efficiency of 55.2% at 850 °C [82]. Binotti et al. [83] also arrived at similar findings, indicating further that the recompression with main compression intercooling S-CO_2 cycle could attain a solar-to-electric efficiency of 24.5%. The studies mentioned previously relied on steady-state design conditions. However, other researchers have conducted dynamic analyses of S-CO_2 CSP performance with varied solar irradiance levels during different seasons, including spring, summer, fall and winter [84,85]. More research conducted by researchers to assess the performance of S-CO_2 CSP power systems has been summarized and presented in Table 9. Despite the extensive analysis conducted on the feasibility and efficacy of the S-CO_2 CSP solar power system, its implementation on a commercial scale has not yet been achieved due to the challenges associated with operating under high-temperature and high-pressure conditions, which are necessary for optimal performance and analysis. Attaining and sustaining these conditions can pose difficulties to material selection and component production. In addition, the initial capital cost may exhibit a considerably higher magnitude in comparison to alternative

renewable energy sources and technologies such as PV panels or conventional fossil fuel power plants.
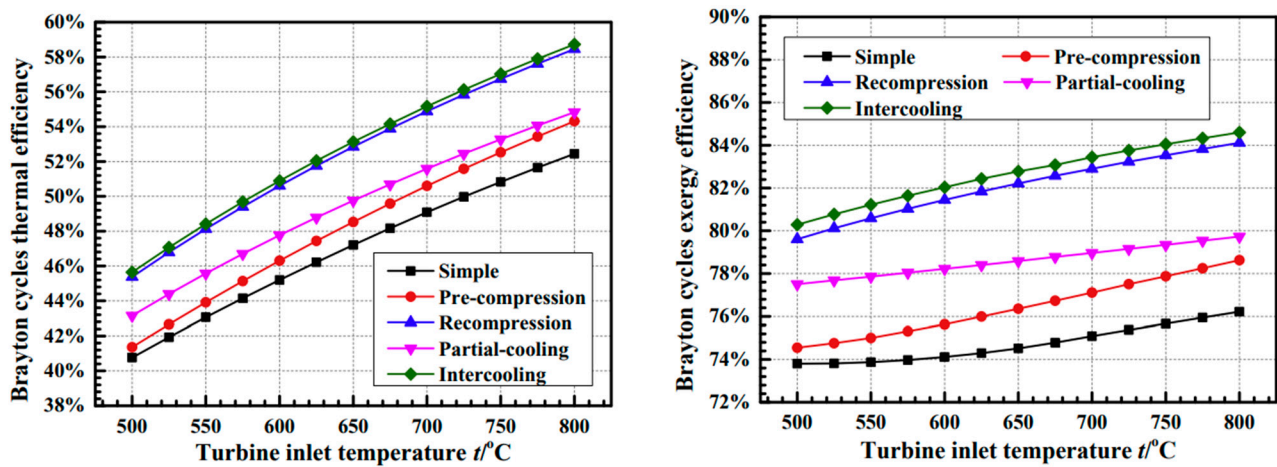

Figure 13. Variations in thermal and exergy efficiency with different turbine inlet temperatures for five S-CO$_2$ CSP cycles [81].

Table 9. Summary of typical applications of S-CO$_2$ in CSP and modelling/experimental analysis.

Ref.	Year	Approach	CSP type	Thermodynamic Cycles	P$_{max}$ (MPa)	P$_{min}$ (MPa)	T$_H$ (°C)	T$_L$ (°C)	η$_{th}$	W$_{net}$ (MW)
Dyreby et al. [85]	2013	Modelling	-	Recuperation; Recompression	25	8.14~9.17	700	45	47.6~49.4%	10
Iverson et al. [86]	2013	Experiment	Six immersion heaters	Split-flow recompression	14.091	7.688	538	32.4	15.2%	0.176
Neises and Turchi [80]	2014	Modelling	Solar power tower	Recuperation; Recompression; Partial Cooling	25		650	50	44.6~49.5%	35
Padilla et al. [82]	2015	Modelling	Solar power tower	Recuperation; Recompression; Partial cooling with recompression; Recompression with main compression intercooling	25	6.25~16.1	500~800	55.5	35.1~55.2%	-
Osorio et al. [84]	2016	Modelling	Solar power tower	Recompression with multi-stage expansion and intercooling	20	8	497.1~515.2	38.2~44.9	44.3~48.1%	1.516~1.855
Binotti et al. [83]	2017	Modelling	molten salts solar tower plants	Recompression; Partial-cooling; Recompression with main compression intercooling	25	5.23~9.37	740~780	51	-	23.81~24.78
Wang et al. [53,79,81]	2017	Modelling	Molten salt solar power towers	Recompression; Intercooling; Partial-cooling; Split-expansion	25	7.6	450~800	35	38%~58%	1
Khan et al. [87]	2019	Modelling	Parabolic dish solar	Recompression with reheat	20	7.6	549.9	31.85	33.7%	-
Sun et al. [88]	2019	Experiment	Heater	Recuperation with spray-assisted dry cooling	20	8	610	42~57	39.4~40.9%	0.79~0.9
Liu et al. [89]	2021	Modelling	Molten salt solar power tower	Split-recompression with bottom Rankine Cycle	31.81	8.14	893.2	35	44.5~49.5%	50
Chen et al. [90]	2023	Modelling	-	Recompression	25	7.615~7.646	500~700	32	44.5~53.7%	-

5.3. S-CO$_2$ Cycle for Geothermal Power Systems

Geothermal power generation is the utilization of underground thermal energy to generate electricity. In general, brine is the most common working fluid to extract heat from underground earth and convert it into electricity via thermodynamic power cycles. However, conventional geothermal energy conversion systems are constrained by size and location, while brines have the potential for scaling and erosion of injection systems and heat exchangers. Therefore, improved monitoring and system management are essential [91]. Furthermore, the majority of geothermal energy is trapped within rocks characterized by low fracture permeability and a lack of fluid circulation. Consequently, the development of new technologies is imperative.

To extract energy from hard dry rock (HDR) to generate electricity, enhanced geothermal systems (EGS) involve the extraction of thermal energy via the creation of artificial geothermal reservoirs [92]. Typically, an EGS requires hydrofracturing of rock with low natural permeability [93]. The performance of EGS based on working fluid of CO$_2$ and water was investigated, and it was found that a CO$_2$-EGS was more efficient than a water-EGS [94–97]. A CO$_2$-Plume Geothermal (CPG) system was proposed by Randolph et al. [98], as shown in Figure 14, CO$_2$ was sent to the subsurface to recover the energy, and then a small portion of it was piped back to the surface to undergo turbine, generator and heat exchangers for electricity generation, or it was used to provide heat for a power cycle. A CPG was applied as an alternative technology to EGS without hydrofracturing, and the amount of CO$_2$ stored in a CO$_2$-CPG system was significantly greater than what was typically seen in CO$_2$-EGS [93]. Adams et al. [99] conducted a comprehensive comparison between CPG and brine geothermal systems under the conditions of different reservoirs. The results showed that in comparison to brine systems, CO$_2$ direct systems generated a higher net power output when dealing with reservoir depths and permeabilities that fall within the low to moderate range. Wang [92] compared the performance of different S-CO$_2$ cycles, including pre-compression, inter-cooling and reheating for utilizing geothermal energy via model simulations. Subsequently, the S-CO$_2$ Cycle with reheating has the highest net power output of 6.9 MW. Similarly, with low-grade geothermal heat sources, Ruiz-Casanova et al. [100] numerically analyzed the performance of four S-CO$_2$ Brayton cycles, including simple, recuperation, intercooling and intercooled recuperation. The results revealed that the intercooled recuperated Brayton cycle achieved the best performance with the highest power output and highest thermal efficiency. Furthermore, an enhanced natural gas recovery (EGR) reservoir has a larger size than an EGS reservoir, and EGR-CPG can be a promising technology to efficiently extract heat from geothermal. In order to enhance the total producible energy from the gas field while mitigating electricity costs, Ezekiel et al. [101] explored the potential of CPG and the enhanced natural gas recovery (EGR) in a high-temperature reservoir using S-CO$_2$ thermodynamic cycles, as depicted in Figure 15. In this process, external CO$_2$ was introduced into the deep natural gas reservoir. As it travels from the injection well to the production well, the CO$_2$ fluid undergoes heating due to the presence of hot natural gas. The resulting mixture of high-temperature gases was then transported to the land surface, where they were separated for use in a combined system consisting of an S-CO$_2$ cycle and an ORC. The simulation results demonstrated that under conditions of a low CO$_2$ circulation rate in the CPG stage, a net electricity generation of 0.656 MWe could be sustained over 42 years. Conversely, when the CO$_2$ circulation rate is high, the system could generate 1.187 MWe over a period of 32 years. The higher flow rate of CO$_2$ contributed to higher power output with less timeframe and thus fewer capital costs could be achieved. In addition to the investigation of different S-CO$_2$ configurations, researchers also carried out the comparison between pure CO$_2$ and CO$_2$ mixtures. Wright et al. [102] developed an S-CO$_2$ cycle for low-temperature geothermal heat sources and conducted a system performance comparison when either CO$_2$-mixture (CO$_2$/butane) or pure CO$_2$ as a working fluid. The findings indicated that, at a turbine inlet temperature of 160 °C and a dry heat rejection temperature of 46.7 °C, the efficiency of the CO$_2$-mixture cycle was 18.1%, while the efficiency of the pure CO$_2$ cycle was 15%. Another investigation

on CO_2 mixture containing SF6 was conducted by Yin et al. [103]. It was observed that CO_2 concentrations of 15 mol% led to the highest Brayton cycle efficiency, while 20 mol% resulted in the highest Rankine cycle efficiency. Some recent S-CO_2 geothermal systems studies are listed in Table 10.

While geothermal energy is characterized by its cleanliness, sustainability and low operating costs, its utilization is constrained by geographic factors. Only a few countries with ample geothermal resources can effectively harness this energy source. The construction of a geothermal power plant demands substantial initial investments since the drilling and exploration stages are the main project-related risks. Additionally, when assessing a technology's potential, the technology readiness level (TRL) is often utilized [104]. Although S-CO_2-CPG demonstrates superior thermal performance compared to conventional hydrothermal geothermal power systems, it is important to note that the TRL of CO_2-CPG is relatively low and less mature in comparison to traditional approaches.
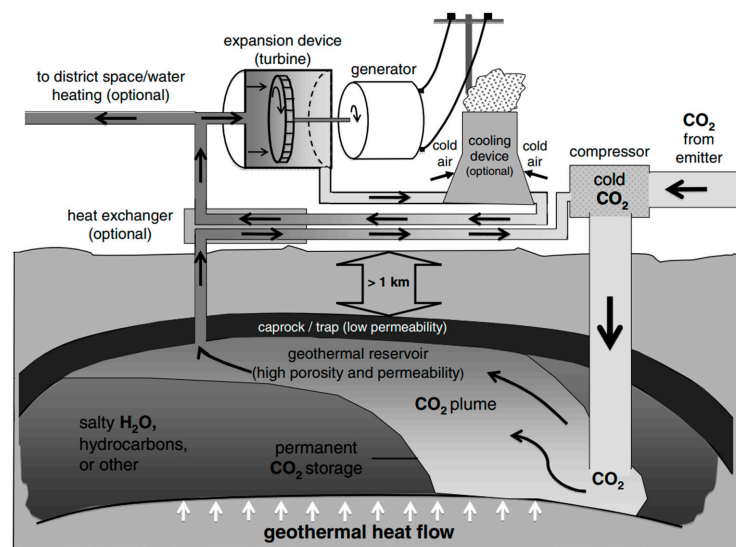

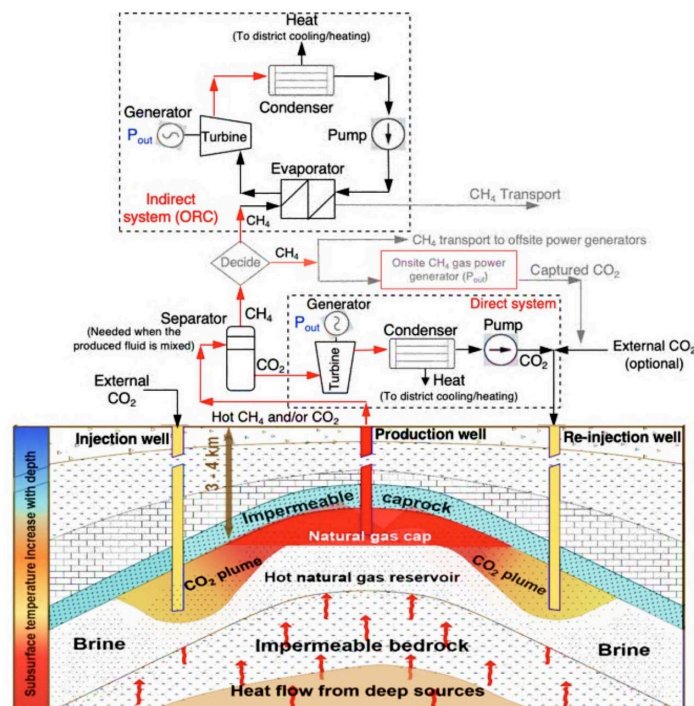**Figure 14.** Simplified schematic of a CO_2-plume geothermal (CPG) system [98].

Figure 15. The integrated CO_2 EGR-CPG system designed for electricity generation [101].

Table 10. S-CO$_2$ geothermal systems studies in recent years.

| Ref.	Year	Technology		Tsource (°C)	P$_{max}$ (MPa)	P$_{min}$ (Mpa)	W$_{net}$ (kW)	η$_{th}$
Ezekiel et al. [101]	2019	CO$_2$ EGR-CPG		150	30		1187	
Ruiz-Casanova et al. [100]	2020	Simple Brayton cycle		150	23.942	7.904	725.34	10.71%
		Recuperated Brayton cycle			17.919	8	748.95	11.1%
		Intercooled Brayton cycle			24.74	7.939	719.31	10.62%
		Intercooled recuperated Brayton cycle			18.332	8.13	779.99	11.51%
Wang [92]	2018	Simply sCO$_2$ cycle		195	22.5	7.8	2758	13.92%
		Recuperative sCO$_2$ cycle					2584	8.92%
		sCO$_2$ cycle with pre-compression and inter-cooling					3194	11.02%
		sCO$_2$ cycle with reheating					5970	10.3%
		sCO$_2$ Cycle with pre-compression, inter-cooling and reheating					6904	11.91%
Wright [102]	2017	sCO$_2$ cycle with recompression, reheating and intercooling		>160	22.2	8.62	2369	15%
		sCO$_2$/10% Butane cycle with recompression, reheating and intercooling					2675	18%
Glos et al. [105]	2019	s-CO$_2$ Rankine cycle		>102	24.5	6	3240	5%
Levy et al. [106]	2018	Direct turbine expansion system		225	14.5	8.34	30,000	-
Tagliaferri et al. [107]	2022	Direct sCO$_2$ cycle Indirect sCO$_2$ cycle with ORC (binary cycle)		District heating system located between turbine: T hot water = 35 °C T cold water = 60 °C Recovery heat exchanger located after the production well: T hot water = 50 °C T cold water = 80 °C 35 °C ≤ T$_{injection}$ ≤ 55 °C			1630 2612	- -
		Direct S-CO$_2$ with cogeneration	District heating system located between turbine stages				1556	-
			District heating system located after the production well				1055	-
		Combined direct sCO$_2$ with ORC	Recovery heat exchanger located before the injection well				2918	-
			Recovery heat exchanger located after the production well				2663	-
Sun et al. [108]	2023	T-CO$_2$ Rankine Cycle + power and heat generation unit		1966	20	5.73	67.5	42.5%

5.4. S-CO$_2$ Cycle for Waste Heat Recovery

Plenty of waste heat exists in industries, which can be potentially recovered, as shown in Table 11. Waste heat recovery represents a promising approach for minimizing energy consumption and channelling additional energy towards end-use applications. Given the substantial abundance of waste heat in process industries, advanced thermodynamic cycles present greater potential to increase power generation and improve energy efficiency [109].

Table 11. Waste heat sources and end uses [110].

Waste Heat Sources	Energy End Use
• Combustion exhausts: Glass melting furnace; Cement kiln; Fume incinerator; Aluminum reverberatory furnace; Boiler. • Process off-gas: Steel electric arc furnace. • Cooling water from Furnaces; Air compressors; Internal combustion engines. • Conductive, convective and radiative losses from equipment and heat products	• Combustion air preheating; • Boiler feedwater preheating; • Load preheating; • Power generation; • Steam generation for use in power generation; mechanical power; process steam; • Space heating; • Water preheating; • Transfer to liquid or gaseous process streams.

Waste heat to power (WHP) involves harnessing the heat that is typically wasted by an ongoing process and converting it into electrical energy. The primary conversion route is shown in Figure 16, with applicable technologies and thermodynamic cycles such as steam Rankine, ORC, Stirling, Kalina, and S-CO$_2$ Brayton, as shown in Figure 17. As the S-CO$_2$ Brayton cycle outperforms the existing Rankine cycles in terms of adapting for higher grade heat sources, higher efficiency, system compactness and environmentally friendly working fluid, it has been considered in numerous applications, including waste heat recovery. The initial commercial implementation of a supercritical CO$_2$ power cycle emerged in Alberta. This system captured residual heat from a gas-fired turbine and subsequently transformed this heat into electricity utilizing an innovative S-CO$_2$ power cycle based on the patented technology developed by Echogen and General Electric [111,112], as shown in Figure 18. The power generation system consists of two cycles: a gas turbine cycle and a steam Rankine cycle. Typically, the exhaust gas temperature emanating from a gas turbine exceeds 450 °C, and the conventional steam Rankine cycle makes use of this exhaust gas to enhance thermal efficiency. Ahnv et al. [113] conducted research on the application of a basic S-CO$_2$ cycle for recovering waste heat from a gas turbine shipboard. Their study revealed that it was possible to recover 16.7% of the wasted energy. Zhang et al. [114] carried out a novel recompression S-CO$_2$ system to recover the waste heat from an internal combustion engine in which one more heater and one more turbine were added in the cycle to continuously recover the waste heat. Results revealed that the recovery efficiency of this novel system increased by about 18%. Song et al. [115] pointed out that preheating the S-CO$_2$ cycle can improve net power output in the waste heat recovery system. Wright et al. [116] compared the performance of four different layouts of S-CO$_2$ for waste heat recovery from a gas turbine, including simple recuperation, cascaded, dual recuperated and recuperated with preheating Brayton cycles, as shown in Figure 19. The results pointed out that the simple recuperation cycle had the lowest waste recovery efficiency of 61.2%, while the cascaded cycle had the highest efficiency of 85.64%. Nonetheless, the cascaded cycle demonstrates the lowest thermal efficiency and net cycle efficiency, at 26.5% and 24.7%, respectively. In contrast, the simple recuperated cycle attains the highest values, with thermal efficiency and net cycle efficiency reaching 30.42% and 28.3%, respectively. Manente et al. [117] further investigated three other S-CO$_2$ layouts for recovering waste heat of temperature at 600 °C, finding that the S-CO$_2$ duo-expansion cycle had the highest energy conversion efficiency. More research regarding waste heat recovery technologies has been summarized in Table 12.
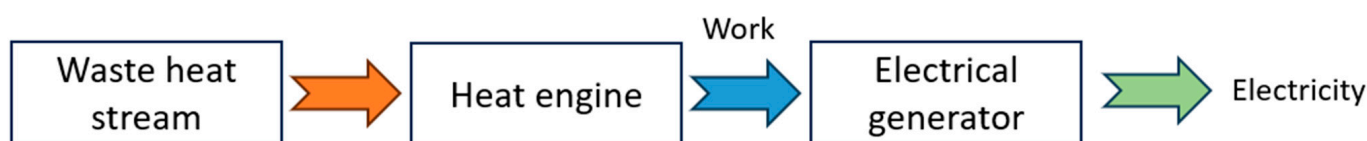
Figure 16. Basic process of a WHP system.

Although waste heat recovery systems are attracting more and more attention, there are limitations due to factors such as temperature constraints and the expenses associated with recovery equipment. The majority of waste heat recovery research focuses on medium temperatures ranging from 230 °C to 650 °C because low temperatures offer limited thermal energy, lower electricity generation and thus lower economic viability. However, recovering high temperatures of waste heat can lead to increased thermal stress on materials used in heat exchangers.
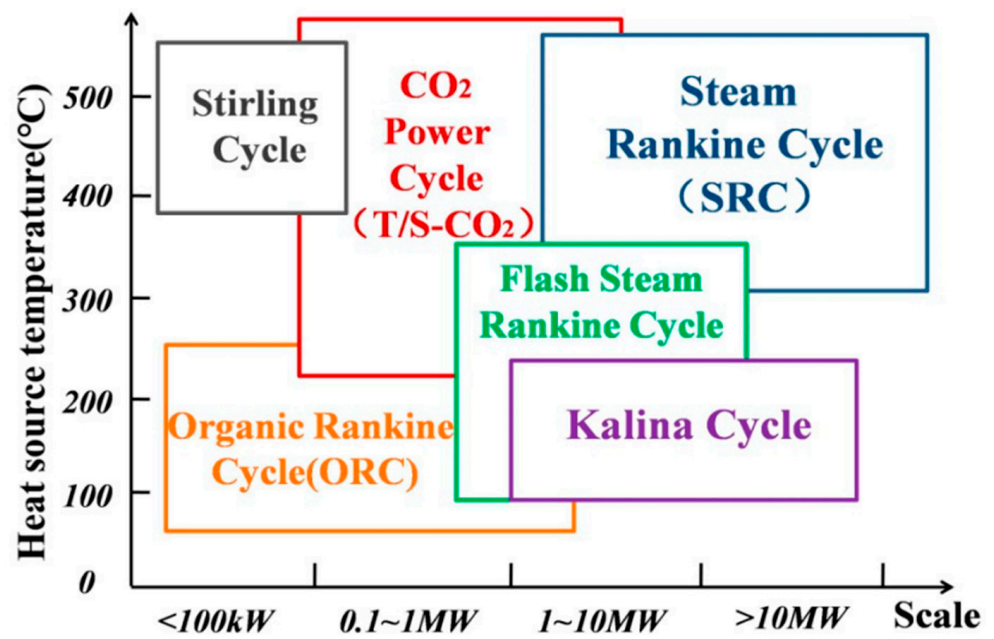
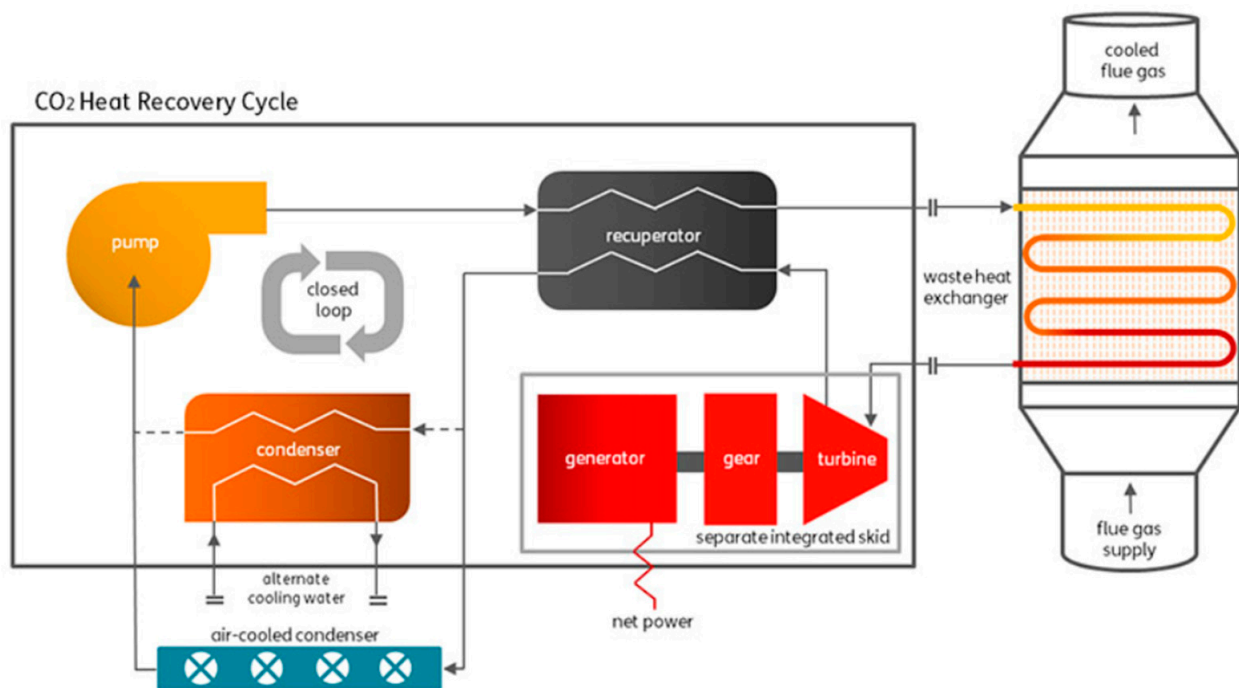**Figure 17.** Thermodynamic cycles for waste heat recovery at different temperatures and scales [118].

Figure 18. A schematic diagram showing waste recovery cycle using supercritical carbon dioxide [111,112].
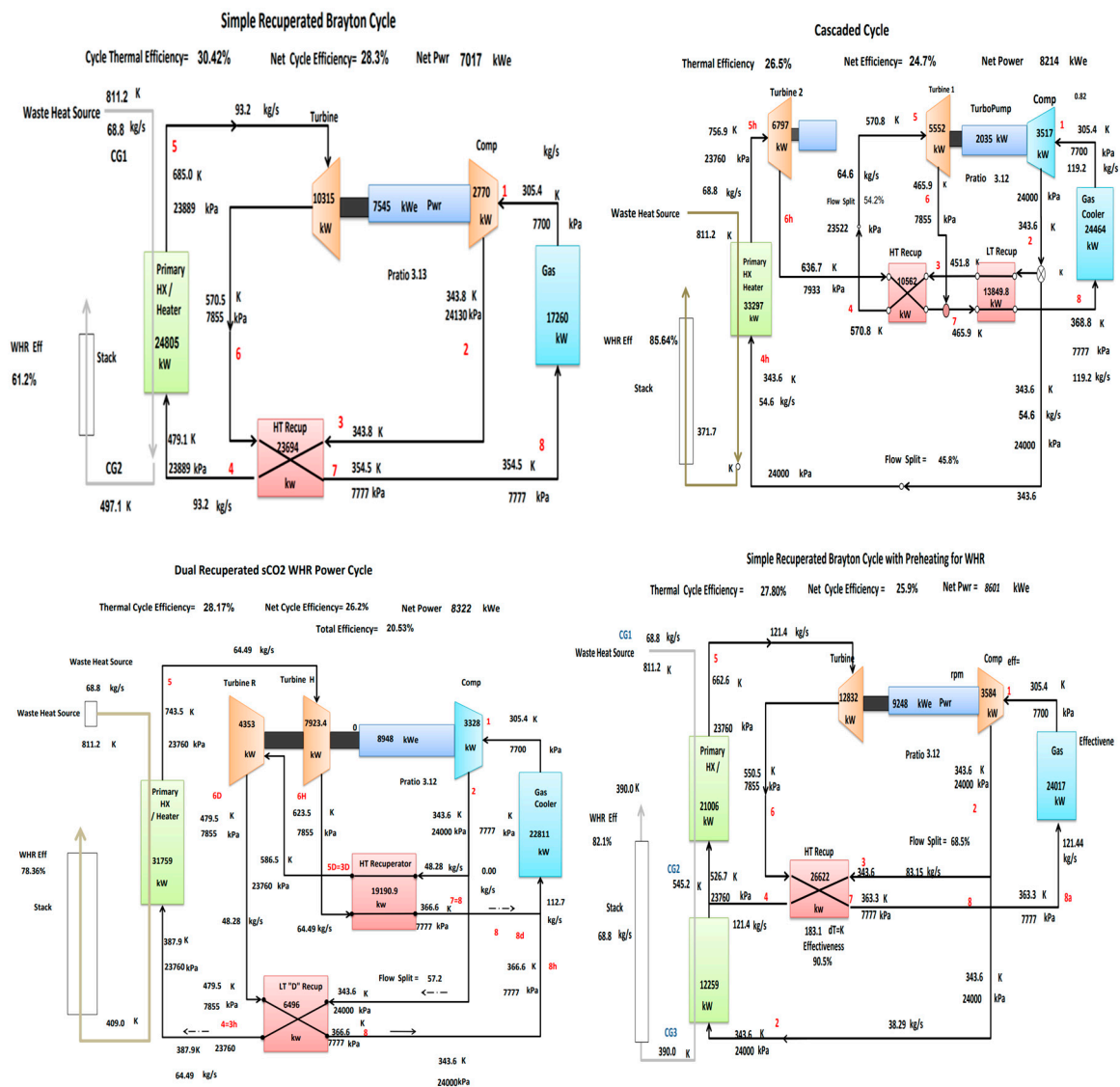
Figure 19. Different layouts of S-CO$_2$ waste heat recovery power systems for gas turbine waste heat recovery [116].

Table 12. Research on waste heat recovery in recent years.

Ref.	Year	Source	Cycle	Power of Source (kW)	T$_{source}$ (°C)	P$_{max}$ (Mpa)	P$_{min}$ (Mpa)	W$_{net}$ (kW)	η_{th}	$\eta_{recovery}$
Ahnb et al. [113]	-	Gas turbine	Recuperation S-CO$_2$	25,000	566	-	-	4175	-	16.70%
Ahmadi et al. [119]	2016	Proton exchange membrane fuel cell	S-CO$_2$ Rankine cycle combined with liquefied natural gas cycle	-	>70	10	0.6	1413	-	66.39%
Wright et al. [116]	2016	Gas turbine	Recuperation S-CO$_2$	40,731	549	24	7.7	7017	30.42%	61.20%
			Cascaded S-CO$_2$ cycle					8214	26.50%	85.64%
			Dual recuperated sCO$_2$					8322	28.17%	78.36%
			Recuperated Brayton cycle with preheating					8601	27.80%	82.10%

Table 12. *Cont.*

Ref.	Year	Source	Cycle	Power of Source (kW)	T_{source} (°C)	P_{max} (Mpa)	P_{min} (Mpa)	W_{net} (kW)	η_{th}	$\eta_{recovery}$
Manjunath et al. [120]	2018	Gas turbine	Recuperation S-CO$_2$ with T-CO$_2$ vapour compression cycle	20,600	572	20	>7.37	3138	38.70%	44.50%
Song et al. [115]	2018	Engine waste heat	Preheating S-CO$_2$	996	300	15	7.8	64	-	-
			Preheating S-CO$_2$ with regeneration					68		
Zhang et al. [114]	2020	Internal combustion engines	Recompression S-CO$_2$	235.8	519	25	8	33.06	35.86%	58.70%
Manente et al. [117]	2020	Steel industry	S-CO$_2$ dual expansion	2010	600	20	7.63	1000	26.62%	22.30%
		Gas turbine	S-CO$_2$ dual recuperation	2312					28.40%	19.39%
		Fuel cell	S-CO$_2$ partial heating	2073					25.82%	21.63%
Bonalumi et al. [121]	2021	Gas turbine	Partial heating S-CO$_2$	4710	511	26	9.56	1550	25%	70%
Sanchez et al. [122]	2011	Molten carbonate fuel cell	Simple recuperation S-CO$_2$	-	>650	22.5	7.5	583.6	39.90%	59.40%
Marchionni et al. [123]	2021	Simulated waste heat source–Air heater	Simple recuperation S-CO$_2$	830	650	20	7.4	84	23%	-
			Reheating S-CO$_2$					87	25%	-
			Recompression S-CO$_2$					85	24%	-
			Recompression reheating S-CO$_2$					88	27%	-
			Preheating S-CO$_2$					155	26%	-
			Preheating Split-Expansion S-CO$_2$					140	23%	-
			Split-heating Split-Expansion S-CO$_2$					110	17.50%	-
			Preheating pre-compression S-CO$_2$					150	25	-

5.5. Barriers to Take Up of the S-CO$_2$ Technology

The application of supercritical CO$_2$ in both power cycles or heating and cooling systems [124–127] have potential advantages in efficiency, size and environmental impact. However, the barriers to taking up this technology can be concluded as follows:

- Although a small power generation system can be constructed owing to the high density of CO$_2$, it allows for more compact turbine, compressor and heat exchanger components. The design, production and selection of turbomachinery is still a challenge for operating CO$_2$ in a wide range of temperatures and pressures.
- Enhancing the efficiency of the system via the improvement in heat exchangers remains a compelling aspect for the successful operation of a S-CO$_2$ Brayton cycle, given the presence of at least two heat exchangers in the basic cycle.
- Insufficient practical experience and performance data from both experimental and commercial applications to provide solid support for applying this technology in the area of renewable energy.

6. Conclusions

The S-CO$_2$ cycle development has attracted considerable attention for its applications in renewable energy sectors. This paper reviews advanced S-CO$_2$ technologies and cycles integrated with renewables such as biomass, solar and geothermal, as well as waste heat

for power generation. The S-CO$_2$ system can achieve higher efficiency compared to other conventional power generation systems, as CO$_2$ working fluid can achieve a more effective thermal match with the applicable heat source. Different renewable energies have been categorized and reviewed according to their characteristics, including temperature ranges, energy conversion routes, and suitable technologies.

Biomass has the capacity to reach temperatures as high as 1400 °C via combustion, while solar energy can achieve temperatures up to 1000 °C, allowing its associated power generation system to achieve higher net power output and enhanced energy conversion efficiency in the range of 0.1~68 MWe by adopting different S-CO$_2$ layouts. By reviewing recent years' studies, thermal efficiencies of S-CO$_2$ biomass systems are in the range of 21~78%, and the S-CO$_2$ solar system is in the range of 15.2~58%. Combined multiple cycles for biomass energy conversion can achieve higher power output. Partial cooling, intercooling and recompression cycles are considered the most favourable cycle configurations for concentrated solar power. The majority of waste heat recovery research focuses on medium temperatures ranging from 230 °C to 650 °C. From the reviewed latest publications, the thermal efficiency and energy conversion efficiency can be achieved in the range of 17.5~39.9% and 18~85%, respectively. The simple recuperation S-CO$_2$ Brayton cycle for waste heat recovery is less attractive due to its lower net power output. In terms of a relatively lower temperature heat source geothermal, supercritical CO$_2$-Plume Geothermal demonstrates superior thermal performance compared to conventional hydrothermal geothermal power systems. The thermal efficiency of different S-CO$_2$ Brayton cycles for geothermal utilization ranges from 8.92% to 18%.

Advanced S-CO$_2$ cycles for renewable energy are the promising approach to improve power output and increase thermal efficiency than the conventional Rankine cycle. There are still some barriers that need to be considered. The limited large-scale application of biomass can be attributed to the need for logistics for feedstock collection and transportation, elevated feedstock costs compared to fossil fuels and greater upfront capital investment requirements. The majority of current CSP solar thermal projects worldwide are primarily based on the steam Rankine cycle. This is due to the Rankine cycle being a mature technology with lower initial capital cost compared to the S-CO$_2$ Brayton cycle. Geothermal power plants are more constrained by location, which must be situated in close proximity to or directly above geothermal resources. The effectiveness of waste heat recovery is heavily dependent on the temperature of the waste heat source. Waste heat recovery faces limitations due to factors such as temperature constraints and the expenses associated with recovery equipment. Moreover, there is a pronounced need for the advancement of turbomachinery and heat exchanger technology. Future research on S-CO$_2$ renewable energy power generation systems is expected to focus on achieving both economic viability and high efficiency.

Nomenclature

Cp	Specific heat at constant pressure, J/(kg.K)
h	Enthalpy, J/kg
$\dot{m}$	Mass flow rate, kg/s
P	Pressure, Pa
Q	Heat transfer, W
T	Temperature, K
W	Power, W
Greek letters	
η	Efficiency
ε	Effectiveness
Subscripts	
C	Cooler
H	Heater, High
L	Low
P	Compressor
Rec	Recuperator
s	Isentropic
th	Thermal
T	Turbine

References

1. Energy Institute. *Statistical Review of World Energy*; Energy Institute: London, UK, 2023.
2. Schuster, A.; Karellas, S.; Kakaras, E.; Spliethoff, H. Energetic and Economic Investigation of Organic Rankine Cycle Applications. *Appl. Therm. Eng.* **2009**, *29*, 1809–1817. [CrossRef]
3. Tchanche, B.F.; Lambrinos, G.; Frangoudakis, A.; Papadakis, G. Low-Grade Heat Conversion into Power Using Organic Rankine Cycles—A Review of Various Applications. *Renew. Sustain. Energy Rev.* **2011**, *15*, 3963–3979. [CrossRef]
4. Coco-Enríquez, L.; Muñoz-Antón, J.; Martínez-Val, J.M. New Text Comparison between CO_2 and Other Supercritical Working Fluids (Ethane, Xe, CH_4 and N_2) in Line- Focusing Solar Power Plants Coupled to Supercritical Brayton Power Cycles. *Int. J. Hydrogen Energy* **2017**, *42*, 17611–17631. [CrossRef]
5. Manzolini, G.; Binotti, M.; Bonalumi, D.; Invernizzi, C.; Iora, P. CO_2 Mixtures as Innovative Working Fluid in Power Cycles Applied to Solar Plants. Techno-Economic Assessment. *Sol. Energy* **2019**, *181*, 530–544. [CrossRef]
6. Besarati, S.M.; Yogi Goswami, D. Analysis of Advanced Supercritical Carbon Dioxide Power Cycles with a Bottoming Cycle for Concentrating Solar Power Applications. *J. Sol. Energy Eng.* **2013**, *136*, 010904. [CrossRef]
7. Sulzer, G. Verfahren zur erzeugung von arbeit aus warme. *Swiss Pat.* **1950**, *269599*, 15.
8. Feher, E.G. The supercritical thermodynamic power cycle. *Energy Convers.* **1968**, *8*, 85–90. [CrossRef]
9. Angelino, G. Perspectives for the Liquid Phase Compression Gas Turbine. *J. Eng. Power* **1967**, *89*, 229–236. [CrossRef]
10. Angelino, G. Carbon Dioxide Condensation Cycles for Power Production. *J. Eng. Power* **1968**, *90*, 287–295. [CrossRef]
11. Angelino, G. Real Gas Effects in Carbon Dioxide Cycles. In Proceedings of the ASME 1969 Gas Turbine Conference and Products Show, Cleveland, OH, USA, 9–13 March 1969. [CrossRef]
12. Brun, K.; Friedman, P.; Dennis, R. *Fundamentals and Applications of Supercritical Carbon Dioxide (SCO₂) Based Power Cycles*; Woodhead Publishing: Cambridge, UK, 2017.
13. Le Moullec, Y. Conceptual Study of a High Efficiency Coal-Fired Power Plant with CO_2 Capture Using a Supercritical CO_2 Brayton Cycle. *Energy* **2013**, *49*, 32–46. [CrossRef]
14. Mecheri, M.; Le Moullec, Y. Supercritical CO_2 Brayton Cycles for Coal-Fired Power Plants. *Energy* **2016**, *103*, 758–771. [CrossRef]
15. Xu, J.; Wang, X.; Sun, E.; Li, M. Economic Comparison between SCO₂ Power Cycle and Water-Steam Rankine Cycle for Coal-Fired Power Generation System. *Energy Convers. Manag.* **2021**, *238*, 114150. [CrossRef]
16. Wang, Z.; Xu, J.; Wang, T.; Miao, Z.; Wang, Q.; Liu, G. Performance of SCO₂ Coal-Fired Power Plants at Various Power Capacities. *J. Clean. Prod.* **2023**, *416*, 137949. [CrossRef]
17. Ahn, Y.; Bae, S.J.; Kim, M.; Cho, S.K.; Baik, S.; Lee, J.I.; Cha, J.E. Review of Supercritical CO_2 Power Cycle Technology and Current Status of Research and Development. *Nucl. Eng. Technol.* **2015**, *47*, 647–661. [CrossRef]
18. Dostal, V.; Driscoll, M.J.; Hejzlar, P. A Supercritical Carbon Dioxide Cycle for Next Generation Nuclear Reactors. Doctoral Dissertation, Department of Nuclear Engineering, Massachusetts Institute of Technology, Cambridge, MA, USA, 2004.
19. Moisseytsev, A.; Sienicki, J.J. Investigation of Alternative Layouts for the Supercritical Carbon Dioxide Brayton Cycle for a Sodium-Cooled Fast Reactor. *Nucl. Eng. Des.* **2009**, *239*, 1362–1371. [CrossRef]
20. Wright, S.A.; Conboy, T.M.; Radel, R.; Rochau, G.E. *Modeling and Experimental Results for Condensing Supercritical CO₂ Power Cycles*; OSTI OAI (U.S. Department of Energy Office of Scientific and Technical Information): Oak Ridge, TN, USA, 2011. [CrossRef]

21. Yoon, H.J.; Ahn, Y.; Lee, J.I.; Addad, Y. Potential Advantages of Coupling Supercritical CO_2 Brayton Cycle to Water Cooled Small and Medium Size Reactor. *Nucl. Eng. Des.* **2012**, *245*, 223–232. [CrossRef]
22. World Nuclear Performance Report 2023. Available online: https://www.world-nuclear.org/getmedia/0156a8d7-01c6-42d9-97be-3f04f34cb8fa/performance-report-2023-final.pdf.aspx (accessed on 1 September 2023).
23. Kumar, P.; Srinivasan, K. Carbon Dioxide Based Power Generation in Renewable Energy Systems. *Appl. Therm. Eng.* **2016**, *109*, 831–840. [CrossRef]
24. Crespi, F.; Gavagnin, G.; Sánchez, D.; Martínez, G.S. Supercritical Carbon Dioxide Cycles for Power Generation: A Review. *Appl. Energy* **2017**, *195*, 152–183. [CrossRef]
25. Marchionni, M.; Bianchi, G.; Tassou, S.A. Review of Supercritical Carbon Dioxide (SCO_2) Technologies for High-Grade Waste Heat to Power Conversion. *SN Appl. Sci.* **2020**, *2*, 611. [CrossRef]
26. White, M.T.; Bianchi, G.; Chai, L.; Tassou, S.A.; Sayma, A.I. Review of Supercritical CO_2 Technologies and Systems for Power Generation. *Appl. Therm. Eng.* **2021**, *185*, 116447. [CrossRef]
27. Guo, J.Q.; Li, M.J.; He, Y.L.; Jiang, T.; Ma, T.; Xu, J.L.; Cao, F. A Systematic Review of Supercritical Carbon Dioxide(S-CO_2) Power Cycle for Energy Industries: Technologies, Key Issues, and Potential Prospects. *Energy Convers. Manag.* **2022**, *258*, 115437. [CrossRef]
28. Ge, Y.T.; Tassou, S.A.; Santosa, I.D.; Tsamos, K. Design Optimisation of CO_2 Gas Cooler/Condenser in a Refrigeration System. *Appl. Energy* **2015**, *160*, 973–981. [CrossRef]
29. Dostal, V.; Hejzlar, P.; Driscoll, M.J. The Supercritical Carbon Dioxide Power Cycle: Comparison to Other Advanced Power Cycles. *Nucl. Technol.* **2006**, *154*, 283–301. [CrossRef]
30. Garg, P.; Kumar, P.; Srinivasan, K. Supercritical Carbon Dioxide Brayton Cycle for Concentrated Solar Power. *J. Supercrit. Fluids* **2013**, *76*, 54–60. [CrossRef]
31. Chen, H.; Goswami, D.Y.; Stefanakos, E.K. A Review of Thermodynamic Cycles and Working Fluids for the Conversion of Low-Grade Heat. *Renew. Sustain. Energy Rev.* **2010**, *14*, 3059–3067. [CrossRef]
32. Chen, Y.; Lundqvist, P.; Johansson, A.; Platell, P. A Comparative Study of the Carbon Dioxide Transcritical Power Cycle Compared with an Organic Rankine Cycle with R123 as Working Fluid in Waste Heat Recovery. *Appl. Therm. Eng.* **2006**, *26*, 2142–2147. [CrossRef]
33. Basu, P. *Biomass Gasification, Pyrolysis and Torrefaction: Practical Design and Theory*; Elsevier Academic Press: London, UK, 2018.
34. Pospíšil, J.; Lisý, M.; Špiláček, M. Optimalization of Afterburner Channel in Biomass Boiler Using CFD Analysis. *Acta Polytech.* **2016**, *56*, 379–387. [CrossRef]
35. Biomass Strategy. 2023. Available online: https://assets.publishing.service.gov.uk/government/uploads/system/uploads/attachment_data/file/1178897/biomass-strategy-2023.pdf (accessed on 1 September 2023).
36. Aboelwafa, O.; Fateen, S.E.K.; Soliman, A.; Ismail, I.M. A Review on Solar Rankine Cycles: Working Fluids, Applications, and Cycle Modifications. *Renew. Sustain. Energy Rev.* **2018**, *82*, 868–885. [CrossRef]
37. Global Solar Energy Share in Electricity Mix. 2022. Statista. Available online: https://www.statista.com/statistics/1302055/global-solar-energy-share-electricity-mix/ (accessed on 1 September 2023).
38. Tzivanidis, C.; Bellos, E.; Antonopoulos, K.A. Energetic and Financial Investigation of a Stand-Alone Solar-Thermal Organic Rankine Cycle Power Plant. *Energy Convers. Manag.* **2016**, *126*, 421–433. [CrossRef]
39. Tchanche, B.F.; Pétrissans, M.; Papadakis, G. Heat Resources and Organic Rankine Cycle Machines. *Renew. Sustain. Energy Rev.* **2014**, *39*, 1185–1199. [CrossRef]
40. Turchi, C.S.; Ma, Z.; Neises, T.W.; Wagner, M.J. Thermodynamic Study of Advanced Supercritical Carbon Dioxide Power Cycles for Concentrating Solar Power Systems. *J. Sol. Energy Eng.* **2013**, *135*, 041007. [CrossRef]
41. Caccia, M.; Tabandeh-Khorshid, M.; Itskos, G.; Strayer, A.R.; Caldwell, A.S.; Pidaparti, S.; Singnisai, S.; Rohskopf, A.D.; Schroeder, A.M.; Jarrahbashi, D.; et al. Ceramic–Metal Composites for Heat Exchangers in Concentrated Solar Power Plants. *Nature* **2018**, *562*, 406–409. [CrossRef] [PubMed]
42. Patil, V.R.; Kiener, F.; Grylka, A.; Steinfeld, A. Experimental Testing of a Solar Air Cavity-Receiver with Reticulated Porous Ceramic Absorbers for Thermal Processing at above 1000 °C. *Sol. Energy* **2021**, *214*, 72–85. [CrossRef]
43. Mahlia, T.M.I.; Syaheed, H.; Abas, A.E.P.; Kusumo, F.; Shamsuddin, A.H.; Ong, H.C.; Bilad, M.R. Organic Rankine Cycle (ORC) System Applications for Solar Energy: Recent Technological Advances. *Energies* **2019**, *12*, 2930. [CrossRef]
44. Loni, R.; Mahian, O.; Najafi, G.; Sahin, A.Z.; Rajaee, F.; Kasaeian, A.; Mehrpooya, M.; Bellos, E.; le Roux, W.G. A Critical Review of Power Generation Using Geothermal-Driven Organic Rankine Cycle. *Therm. Sci. Eng. Prog.* **2021**, *25*, 101028. [CrossRef]
45. DiPippo, R. *Geothermal Power Plants*; Butterworth-Heinemann: Oxford, UK, 2012.
46. Liu, Q.; Duan, Y.; Yang, Z. Performance Analyses of Geothermal Organic Rankine Cycles with Selected Hydrocarbon Working Fluids. *Energy* **2013**, *63*, 123–132. [CrossRef]
47. Quoilin, S.; Broek, M.V.D.; Declaye, S.; Dewallef, P.; Lemort, V. Techno-Economic Survey of Organic Rankine Cycle (ORC) Systems. *Renew. Sustain. Energy Rev.* **2013**, *22*, 168–186. [CrossRef]
48. Reddy, C.; Naidu, S.V.; Rangaiah, G.P. Waste heat recovery methods and technologies: There is significant potential for recovering some of the wasted heat in the CPI. Key requirements, benefits and drawbacks for numerous techniques are reviewed. *Chem. Eng.* **2013**, *120*, 28–39.

49. Wu, P.; Ma, Y.; Gao, C.; Liu, W.; Shan, J.; Huang, Y.-P.; Wang, J.; Zhang, D.; Ran, X. A Review of Research and Development of Supercritical Carbon Dioxide Brayton Cycle Technology in Nuclear Engineering Applications. *Nucl. Eng. Des.* **2020**, *368*, 110767. [CrossRef]

50. Yun, S.; Zhang, D.; Li, X.; Zhou, X.; Jiang, D.; Lv, X.; Wu, W.; Feng, Z.; Min, X.; Tian, W.; et al. Design, Optimization and Thermodynamic Analysis of SCO_2 Brayton Cycle System for FHR. *Prog. Nucl. Energy* **2023**, *157*, 104593. [CrossRef]

51. Khan, Y.; Mishra, R.S. Performance Evaluation of Solar Based Combined Pre-Compression Supercritical CO_2 Cycle and Organic Rankine Cycle. *Int. J. Green Energy* **2020**, *18*, 172–186. [CrossRef]

52. Li, M.J.; Zhu, H.H.; Guo, J.Q.; Wang, K.; Tao, W.Q. The Development Technology and Applications of Supercritical CO_2 Power Cycle in Nuclear Energy, Solar Energy and Other Energy Industries. *Appl. Therm. Eng.* **2017**, *126*, 255–275. [CrossRef]

53. Wang, K.; Li, M.J.; Guo, J.Q.; Li, P.; Liu, Z.B. A Systematic Comparison of Different S-CO_2 Brayton Cycle Layouts Based on Multi-Objective Optimization for Applications in Solar Power Tower Plants. *Appl. Energy* **2018**, *212*, 109–121. [CrossRef]

54. Saeed, M.; Kim, M.H. A Newly Proposed Supercritical Carbon Dioxide Brayton Cycle Configuration to Enhance Energy Sources Integration Capability. *Energy* **2022**, *239*, 121868. [CrossRef]

55. Biomass Co-Firing: A Renewable Alternative for Utilities. 2000. Available online: https://www.nrel.gov/docs/fy00osti/28009.pdf (accessed on 1 September 2023).

56. Biomass for Power Generation and CHP. 2007. Available online: https://iea.blob.core.windows.net/assets/1028bee0-2da1-4d68-8b0a-9e5e03e93690/essentials3.pdf (accessed on 1 September 2023).

57. Liu, H.; Shao, Y.; Li, J. A Biomass-Fired Micro-Scale CHP System with Organic Rankine Cycle (ORC)—Thermodynamic Modelling Studies. *Biomass Bioenergy* **2011**, *35*, 3985–3994. [CrossRef]

58. Qiu, G.; Shao, Y.; Li, J.; Liu, H.; Riffat, S.B. Experimental Investigation of a Biomass-Fired ORC-Based Micro-CHP for Domestic Applications. *Fuel* **2012**, *96*, 374–382. [CrossRef]

59. Chitsaz, A.; Khalilarya, S.; Mojaver, P. Supercritical CO_2 Utilization in a CO_2 Zero Emission Novel System for Bio-Synthetic Natural Gas, Power and Freshwater Productions. *J. CO2 Util.* **2022**, *59*, 101947. [CrossRef]

60. Cao, Y.; Dhahad, H.A.; Rajhi, A.A.; Alamri, S.; Anqi, A.E.; El-Shafay, A.S. Combined Heat and Power System Based on a Proton Conducting SOFC and a Supercritical CO_2 Brayton Cycle Triggered by Biomass Gasification. *Int. J. Hydrogen Energy* **2022**, *47*, 5439–5452. [CrossRef]

61. Ji-chao, Y.; Sobhani, B. Integration of Biomass Gasification with a Supercritical CO_2 and Kalina Cycles in a Combined Heating and Power System: A Thermodynamic and Exergoeconomic Analysis. *Energy* **2021**, *222*, 119980. [CrossRef]

62. Moradi, R.; Cioccolanti, L.; Zotto, L.D.; Renzi, M. Comparative Sensitivity Analysis of Micro-Scale Gas Turbine and Supercritical CO_2 Systems with Bottoming Organic Rankine Cycles Fed by the Biomass Gasification for Decentralized Trigeneration. *Energy* **2023**, *266*, 126491. [CrossRef]

63. Zhang, X.; Ge, Y.; Ling, C.; Lang, P. Power Generation and Heat Recovery from Biomass with Advanced CO_2 Thermodynamic Power Cycles: Modelling Development and Simulation. In Proceedings of the IIR Rankine Conference, Glasgow, UK, 27–31 July 2020.

64. Zhang, X. Experimental and Theoretical Investigation of Biomass-CO_2 Transcritical Brayton Cycles and Heat Exchanger Optimizations. Doctoral Dissertation, London South Bank University, London, UK, 2022.

65. Ge, Y.T.; Zhang, X. Performance Optimization of Supercritical CO_2 Gas Heater in a Biomass-CO_2 Power Generation System. *J. Enhanc. Heat Transf.* **2023**, *30*, 1–28. [CrossRef]

66. Manente, G.; Lazzaretto, A. Innovative Biomass to Power Conversion Systems Based on Cascaded Supercritical CO_2 Brayton Cycles. *Biomass Bioenergy* **2014**, *69*, 155–168. [CrossRef]

67. Wang, X.; Liu, Q.; Bai, Z.; Lei, J.; Jin, H. Thermodynamic Investigations of the Supercritical CO_2 System with Solar Energy and Biomass. *Appl. Energy* **2017**, *227*, 108–118. [CrossRef]

68. Nkhonjera, L.; Ansari, S.H.; Liu, X. Development of Hybrid CSP Biomass Gasification Process with Supercritical Carbon Dioxide Cycle for Power Generation. In Proceedings of the SOLARPACES 2019: International Conference on Concentrating Solar Power and Chemical Energy Systems, Daegu, Republic of Korea, 1–4 October 2019. [CrossRef]

69. Chein, R.Y.; Chen, W.H. Thermodynamic Analysis of Integrated Adiabatic Chemical Looping Combustion and Supercritical CO_2 Cycle. *Energy Convers. Manag. X* **2021**, *10*, 100078. [CrossRef]

70. Wang, Y.; Zhu, L.; He, Y.; Yu, J.; Zhang, C.; Jin, S. High-Efficient and Carbon-Free Biomass Power Generation Hybrid System Consisting of Chemical Looping Air Separation and Semi-Closed Supercritical CO_2 Cycle with a Bottoming Organic Rankine Cycle. *Fuel Process. Technol.* **2022**, *236*, 107393. [CrossRef]

71. Zhang, W.; Chen, F.; Shen, H.; Cai, J.; Yi, L.; Zhang, J.; Wang, X.; Heydarian, D. Design and Analysis of an Innovative Biomass-Powered Cogeneration System Based on Organic Flash and Supercritical Carbon Dioxide Cycles. *Alex. Eng. J.* **2023**, *80*, 623–647. [CrossRef]

72. Zhang, Q.; Chen, H.; Li, B.; Pan, P.; Xu, G.; Zhao, Q.; Jiang, X. A Novel System Integrating Water Electrolysis and Supercritical CO_2 Cycle for Biomass to Methanol. *Appl. Therm. Eng.* **2023**, *225*, 120234. [CrossRef]

73. Concentrating Solar Power Projects. National Renewable Energy Laboratory 2023. Available online: https://solarpaces.nrel.gov/ (accessed on 1 September 2023).

74. Bijarniya, J.P.; Sudhakar, K.; Baredar, P. Concentrated Solar Power Technology in India: A Review. *Renew. Sustain. Energy Rev.* **2016**, *63*, 593–603. [CrossRef]

75. Răboacă, M.S.; Badea, G.; Enache, A.; Filote, C.; Răsoi, G.; Rata, M.; Lavric, A.; Felseghi, R.-A. Concentrating Solar Power Technologies. *Energies* **2019**, *12*, 1048. [CrossRef]

76. He, Y.L.; Qiu, Y.; Wang, K.; Yuan, F.; Wang, W.Q.; Li, M.J.; Guo, J.Q. Perspective of Concentrating Solar Power. *Energy* **2020**, *198*, 117373. [CrossRef]

77. Persichilli, M.; Kacludis, A.; Zdankiewicz, E.; Held, T. Supercritical CO_2 power cycle developments and commercialization: Why sCO2 can displace steam. In Proceedings of the Power-Gen India & Central Asia, New Delhi, India, 19–21 April 2012.

78. Turchi, C. *10 MW Supercritical CO_2 Turbine Test*; OSTI OAI (U.S. Department of Energy Office of Scientific and Technical Information): Oak Ridge, TN, USA, 2014. [CrossRef]

79. Wang, K.; He, Y.L.; Zhu, H.H. Integration between Supercritical CO_2 Brayton Cycles and Molten Salt Solar Power Towers: A Review and a Comprehensive Comparison of Different Cycle Layouts. *Appl. Energy* **2017**, *195*, 819–836. [CrossRef]

80. Neises, T.; Turchi, C. A Comparison of Supercritical Carbon Dioxide Power Cycle Configurations with an Emphasis on CSP Applications. *Energy Procedia* **2014**, *49*, 1187–1196. [CrossRef]

81. Zhu, H.H.; Wang, K.; He, Y.L. Thermodynamic Analysis and Comparison for Different Direct-Heated Supercritical CO_2 Brayton Cycles Integrated into a Solar Thermal Power Tower System. *Energy* **2017**, *140*, 144–157. [CrossRef]

82. Padilla, R.V.; Too, Y.C.S.; Benito, R.; Stein, W. Exergetic Analysis of Supercritical CO_2 Brayton Cycles Integrated with Solar Central Receivers. *Appl. Energy* **2015**, *148*, 348–365. [CrossRef]

83. Binotti, M.; Astolfi, M.; Campanari, S.; Manzolini, G.; Silva, P. Preliminary Assessment of SCO$_2$ Cycles for Power Generation in CSP Solar Tower Plants. *Appl. Energy* **2017**, *204*, 1007–1017. [CrossRef]

84. Osorio, J.D.; Hovsapian, R.; Ordóñez, J.C. Dynamic Analysis of Concentrated Solar Supercritical CO_2-Based Power Generation Closed-Loop Cycle. *Appl. Therm. Eng.* **2016**, *93*, 920–934. [CrossRef]

85. Dyreby, J.J.; Klein, S.A.; Nellis, G.F.; Reindl, D.T. Modeling Off-Design and Part-Load Performance of Supercritical Carbon Dioxide Power Cycles. In *Volume 8: Supercritical CO_2 Power Cycles; Wind Energy; Honors and Awards, Proceedings of the ASME Turbo Expo 2013: Turbine Technical Conference and Exposition, San Antonio, TX, USA, 3–7 June 2013*; ASME: New York, NY, USA, 2013. [CrossRef]

86. Iverson, B.D.; Conboy, T.M.; Pasch, J.J.; Kruizenga, A.M. Supercritical CO_2 Brayton Cycles for Solar-Thermal Energy. *Appl. Energy* **2013**, *111*, 957–970. [CrossRef]

87. Khan, M.S.; Abid, M.; Ali, H.M.; Amber, K.P.; Bashir, M.A.; Javed, S. Comparative Performance Assessment of Solar Dish Assisted S-CO$_2$ Brayton Cycle Using Nanofluids. *Appl. Therm. Eng.* **2019**, *148*, 295–306. [CrossRef]

88. Sun, Y.; Duniam, S.; Guan, Z.; Gurgenci, H.; Dong, P.; Wang, J.; Hooman, K. Coupling Supercritical Carbon Dioxide Brayton Cycle with Spray-Assisted Dry Cooling Technology for Concentrated Solar Power. *Appl. Energy* **2019**, *251*, 113328. [CrossRef]

89. Liu, Y.; Wang, Y.; Zhang, Y.; Hu, S. Design and Performance Analysis of Compressed CO_2 Energy Storage of a Solar Power Tower Generation System Based on the S-CO$_2$ Brayton Cycle. *Energy Convers. Manag.* **2021**, *249*, 114856. [CrossRef]

90. Chen, J.; Cheng, K.; Li, X.; Huai, X.; Dong, H. Thermodynamic Evaluation and Optimization of Supercritical CO_2 Brayton Cycle Considering Recuperator Types and Designs. *J. Clean. Prod.* **2023**, *414*, 137615. [CrossRef]

91. Matek, B. *The Manageable Risks of Conventional Hydrothermal Geothermal Power Systems*; Geothermal Energy Association: Washington, DC, USA, 2014.

92. Wang, X. Investigation of Geothermal Heat Extraction Using Supercritical Carbon Dioxide (sCO$_2$) and Its Utilization in sCO$_2$-based Power Cycles and Organic Rankine Cycles—A Thermodynamic & Economic Perspective. Doctoral Dissertation, Lehigh University, Bethlehem, PA, USA, 2018.

93. Randolph, J.B.; Saar, M.O. Carbon-dioxide plume geothermal (CPG) systems, an alternative engineered geothermal system (EGS) that does not require hydrofracturing: Comparison with traditional EGS regarding geologic reservoir heat energy extraction and potential for inducing seismicity. In *AGU Fall Meeting Abstracts*; American Geophysical Union: Washington, DC, USA, 2010; p. H23I-06.

94. Zhang, F.Z.; Jiang, P.X. Thermodynamic Analysis of a Binary Power Cycle for Different EGS Geofluid Temperatures. *Appl. Therm. Eng.* **2012**, *48*, 476–485. [CrossRef]

95. Mohan, A.R.; Turaga, U.; Shembekar, V.; Elsworth, D.; Pisupati, S.V. Utilization of Carbon Dioxide from Coal-Based Power Plants as a Heat Transfer Fluid for Electricity Generation in Enhanced Geothermal Systems (EGS). *Energy* **2013**, *57*, 505–512. [CrossRef]

96. Xu, T.; Feng, G.; Hou, Z.; Tian, H.; Shi, Y.; Lei, H. Wellbore–Reservoir Coupled Simulation to Study Thermal and Fluid Processes in a CO_2-Based Geothermal System: Identifying Favorable and Unfavorable Conditions in Comparison with Water. *Environ. Earth Sci.* **2015**, *73*, 6797–6813. [CrossRef]

97. Zhong, C.; Xu, T.; Gherardi, F.; Yuan, Y. Comparison of CO_2 and Water as Working Fluids for an Enhanced Geothermal System in the Gonghe Basin, Northwest China. *Gondwana Res.* **2022**, *122*, 199–214. [CrossRef]

98. Randolph, J.B.; Saar, M.O. Coupling Carbon Dioxide Sequestration with Geothermal Energy Capture in Naturally Permeable, Porous Geologic Formations: Implications for CO_2 Sequestration. *Energy Procedia* **2011**, *4*, 2206–2213. [CrossRef]

99. Adams, B.M.; Kuehn, T.H.; Bielicki, J.M.; Randolph, J.B.; Saar, M.O. A Comparison of Electric Power Output of CO_2 Plume Geothermal (CPG) and Brine Geothermal Systems for Varying Reservoir Conditions. *Appl. Energy* **2015**, *140*, 365–377. [CrossRef]

100. Ruiz-Casanova, E.; Rubio-Maya, C.; Pacheco-Ibarra, J.J.; Ambriz-Díaz, V.M.; Romero, C.E.; Wang, X. Thermodynamic Analysis and Optimization of Supercritical Carbon Dioxide Brayton Cycles for Use with Low-Grade Geothermal Heat Sources. *Energy Convers. Manag.* **2020**, *216*, 112978. [CrossRef]

101. Ezekiel, J.; Ebigbo, A.; Adams, B.M.; Saar, M.O. On the use of supercritical carbon dioxide to exploit the geothermal potential of deep natural gas reservoirs for power generation. In Proceedings of the European Geothermal Congress, Hague, The Netherlands, 11–14 June 2019; p. 292.
102. Wright, S.A.; Conboy, T.M.; Ames, D.E. *CO2-Based Mixtures as Working Fluids for Geothermal Turbines*; OSTI OAI (U.S. Department of Energy Office of Scientific and Technical Information): Oak Ridge, TN, USA, 2012. [CrossRef]
103. Yin, H.; Sabau, A.S.; Conklin, J.; McFarlane, J.; Qualls, A.L. Mixtures of SF6–CO2 as Working Fluids for Geothermal Power Plants. *Appl. Energy* **2013**, *106*, 243–253. [CrossRef]
104. De Rose, A.; Buna, M.; Strazza, C.; Olivieri, N.; Stevens, T.; Peeters, L.; Tawil-Jamault, D. *Technology Readiness Level: Guidance Principles for Renewable Energy Technologies*; European Commission: Ispra, Italy, 2017; pp. 17–27. [CrossRef]
105. Glos, S.; Grotkamp, S.; Wechsung, M. Assessment of performance and costs of CO2 based next level geothermal power (NLGP) systems. In Proceedings of the 3rd European Supercritical CO2 Conference, Paris, France, 19–20 September 2019; pp. 19–20. [CrossRef]
106. Levy, E.K.; Wang, X.; Pan, C.; Romero, C.E.; Maya, C.R. Use of Hot Supercritical CO2 Produced from a Geothermal Reservoir to Generate Electric Power in a Gas Turbine Power Generation System. *J. CO2 Util.* **2018**, *23*, 20–28. [CrossRef]
107. Tagliaferri, M.; Gładysz, P.; Ungar, P.; Strojny, M.; Talluri, L.; Fiaschi, D.; Manfrida, G.; Andresen, T.; Sowiżdżał, A. Techno-Economic Assessment of the Supercritical Carbon Dioxide Enhanced Geothermal Systems. *Sustainability* **2022**, *14*, 16580. [CrossRef]
108. Sun, K.; Zhang, W.; Liang, Y.F.; Habila, M.A.; Chen, X.; Zheng, J.; Xie, S.; Project, S. Multi-Variable Investigation of an Innovative Multigeneration Process Based on Geothermal Energy and Allam Power Unit for Yielding Electric Power, Cooling, Heating, and Liquid CO2 with Zero CO2 Footprint. *Sep. Purif. Technol.* **2023**, *326*, 124731. [CrossRef]
109. Hou, S.; Zhou, Y.; Yu, L.; Zhang, F.; Cao, S.; Wu, Y. Optimization of a Novel Cogeneration System Including a Gas Turbine, a Supercritical CO2 Recompression Cycle, a Steam Power Cycle and an Organic Rankine Cycle. *Energy Convers. Manag.* **2018**, *172*, 457–471. [CrossRef]
110. Johnson, I.; Choate, W.T.; Davidson, A. *Waste Heat Recovery. Technology and Opportunities in U.S. Industry*; United States Department of Energy: Washington, DC, USA, 2008. [CrossRef]
111. Lehar, M.A.; Michelassi, V. General Electric Co. System and Method for Recovery of Waste Heat from Dual Heat Sources. U.S. Patent 9,038,391, 26 May 2015.
112. Held, T.J.; Hostler, S.; Miller, J.D.; Vermeersch, M.; Xie, T. Echogen Power Systems LLC. Heat Engine and Heat to Electricity Systems and Methods with Working Fluid Mass Management Control. U.S. Patent 8,613,195, 24 December 2013.
113. Ahnb, Y.; Seoa, H.; Chaa, J.E.; Chunga, H.J. Design of Supercritical CO2 Waste Heat Recovery System for Shipboard Applications. Available online: https://sco2symposium.com/papers2018/098_Paper.pdf (accessed on 1 September 2023).
114. Zhang, R.; Su, W.; Lin, X.; Zhou, N.; Zhao, L. Thermodynamic Analysis and Parametric Optimization of a Novel S-CO2 Power Cycle for the Waste Heat Recovery of Internal Combustion Engines. *Energy* **2020**, *209*, 118484. [CrossRef]
115. Song, J.; Li, X.; Ren, X.; Gu, C. Performance Improvement of a Preheating Supercritical CO2 (S-CO2) Cycle Based System for Engine Waste Heat Recovery. *Energy Convers. Manag.* **2018**, *161*, 225–233. [CrossRef]
116. Wright, S.A.; Davidson, C.S.; Scammell, W.O. Thermo-economic analysis of four sCO2 waste heat recovery power systems. In Proceedings of the Fifth International SCO2 Symposium, San Antonio, TX, USA, 28–31 March 2016.
117. Manente, G.; Costa, M. On the Conceptual Design of Novel Supercritical CO2 Power Cycles for Waste Heat Recovery. *Energies* **2020**, *13*, 370. [CrossRef]
118. Liu, L.; Yang, Q.; Cui, G. Supercritical Carbon Dioxide(S-CO2) Power Cycle for Waste Heat Recovery: A Review from Thermodynamic Perspective. *Processes* **2020**, *8*, 1461. [CrossRef]
119. Ahmadi, M.H.; Mohammadi, A.; Pourfayaz, F.; Mehrpooya, M.; Bidi, M.; Valero, A.; Uson, S. Thermodynamic Analysis and Optimization of a Waste Heat Recovery System for Proton Exchange Membrane Fuel Cell Using Transcritical Carbon Dioxide Cycle and Cold Energy of Liquefied Natural Gas. *J. Nat. Gas Sci. Eng.* **2016**, *34*, 428–438. [CrossRef]
120. Manjunath, K.; Sharma, O.P.; Tyagi, S.K.; Kaushik, S.C. Thermodynamic Analysis of a Supercritical/Transcritical CO2 Based Waste Heat Recovery Cycle for Shipboard Power and Cooling Applications. *Energy Convers. Manag.* **2018**, *155*, 262–275. [CrossRef]
121. Bonalumi, D.; Giuffrida, A.; Sicali, F. Thermo-Economic Analysis of a Supercritical CO2-Based Waste Heat Recovery System. In Proceedings of the E3S Web of Conferences, Strasbourg, France, 5–7 May 2021; Volume 312, p. 08022. [CrossRef]
122. Sanchez, D.; De Escalona, J.M.; Chacartegui, R.; Munoz, A.; Sanchez, T. A Comparison between Molten Carbonate Fuel Cells Based Hybrid Systems Using Air and Supercritical Carbon Dioxide Brayton Cycles with State of the Art Technology. *J. Power Sources* **2011**, *196*, 4347–4354. [CrossRef]
123. Marchionni, M. Supercritical Carbon Dioxide Power Cycles for Waste Heat Recovery Applications. Doctoral Dissertation, Brunel University London, London, UK, 2021.
124. Wang, J.; Belusko, M.; Semsarilar, H.; Evans, M.; Liu, M.; Bruno, F. An Optimisation Study on a Real-World Transcritical CO2 Heat Pump System with a Flash Gas Bypass. *Energy Convers. Manag.* **2022**, *251*, 114995. [CrossRef]
125. Ji, W.; Evans, M.D.; Belusko, M.; Zhao, C.; Liu, M.; Bruno, F. Subcooling Effect on the Optimal Performance for a Transcritical CO2 Heat Pump with Cold Thermal Energy Storage. *Heat Mass Transf.* **2022**, *59*, 1257–1275. [CrossRef]

126. Wang, J.; Belusko, M.; Evans, M.; Liu, M.; Zhao, C.; Bruno, F. A Comprehensive Review and Analysis on CO_2 Heat Pump Water Heaters. *Energy Convers. Manag. X* **2022**, *15*, 100277. [CrossRef]
127. Wang, J.; Belusko, M.; Liu, M.; Semsarilar, H.; Liddle, R.; Alemu, A.; Evans, M.; Zhao, C.; Hudson, J.; Bruno, F. A Comprehensive Study on a Novel Transcritical CO_2 Heat Pump for Simultaneous Space Heating and Cooling—Concepts and Initial Performance. *Energy Convers. Manag.* **2021**, *243*, 114397. [CrossRef]